


 Cite this: *RSC Adv.*, 2021, **11**, 12254

# Medicinal chemistry perspectives of 1,2,3,4-tetrahydroisoquinoline analogs – biological activities and SAR studies

 Faheem,<sup>a</sup> Banoth Karan Kumar,<sup>a</sup> Kondapalli Venkata Gowri Chandra Sekhar,<sup>b</sup> Subhash Chander,<sup>c</sup> Selvaraj Kunjiappan<sup>d</sup> and Sankaranarayanan Murugesan<sup>\*,a</sup>

Isoquinoline alkaloids are a large group of natural products in which 1,2,3,4-tetrahydroisoquinolines (THIQ) form an important class. THIQ based natural and synthetic compounds exert diverse biological activities against various infective pathogens and neurodegenerative disorders. Due to these reasons, the THIQ heterocyclic scaffold has garnered a lot of attention in the scientific community which has resulted in the development of novel THIQ analogs with potent biological activity. The present review provides a much-needed update on the biological potential of THIQ analogs, their structural–activity relationship (SAR), and their mechanism of action. In addition, a note on commonly used synthetic strategies for constructing the core scaffold has also been discussed.

 Received 23rd February 2021  
 Accepted 22nd March 2021

DOI: 10.1039/d1ra01480c

[rsc.li/rsc-advances](http://rsc.li/rsc-advances)

<sup>a</sup>Medicinal Chemistry Research Laboratory, Department of Pharmacy, Birla Institute of Technology and Science-Pilani, Pilani Campus, Pilani-333031, Rajasthan, India. E-mail: [murugesan@pilani.bits-pilani.ac.in](mailto:murugesan@pilani.bits-pilani.ac.in)

<sup>b</sup>Department of Chemistry, Birla Institute of Technology and Science-Pilani, Hyderabad Campus, Jawahar Nagar, Shameerpet Mandal, Medchal Dist., Hyderabad, 500078, Telangana, India

<sup>c</sup>Amity Institute of Phytomedicine and Phytochemistry, Amity University Uttar Pradesh, Noida-201313, India

<sup>d</sup>Department of Biotechnology, Kalasalingam Academy of Research and Education, Krishnankoil-626126, Tamil Nadu, India

## 1. Introduction

1,2,3,4-Tetrahydroisoquinoline (THIQ) is a secondary amine with the chemical formula C<sub>9</sub>H<sub>11</sub>N. The THIQ nucleus containing alkaloids is widely distributed in nature and forms an essential part of the isoquinoline alkaloids family. The THIQ-based antitumor antibiotics isolated from different natural sources have garnered a lot of attention for over 4 decades starting with the isolation of Naphthyrindinomycin **1**. Thereafter, several THIQ antitumor antibiotics belonging to different families such as quinocarcin (quinocarcinol **2**, tetrazomine **3**),



Mr Faheem has a Medicinal Chemistry Graduate degree from the Department of Pharmacy, Birla Institute of Technology, and Science Pilani, Pilani campus, Rajasthan. He completed his Bachelor of Pharmacy at Sri Ramachandra Institute of Higher Education and Research, Tamil Nadu. To his credit, he has published 7 research and review articles in various peer-reviewed journals.

In addition to that, he has also presented 5 papers/posters at various international and national conferences.



Mr Banoth Karan Kumar is currently pursuing his Ph.D. under Dr S. Murugesan at the Department of Pharmacy, Birla Institute of Technology, and Science Pilani, Pilani campus, Rajasthan. Karan has a Pharmaceutical Chemistry Graduate degree from the University College of Pharmaceutical Sciences, Kakatiya University. He has published 14 research and review articles in various

peer-reviewed journals of international and national repute. In addition to that, he has also presented 12 papers/posters at various international and national conferences. His current research area includes synthesis, molecular docking, and dynamics studies for infectious diseases like leishmaniasis.



## Review

saframycins (saframycin A–B 4–5), and naphthyridinomycin (cyanocycline C 6, bioxalomycin  $\alpha_1$  7) have been isolated (Fig. 1). An in-depth review of these antitumor antibiotics has been presented elsewhere.<sup>1</sup>

THIQ containing synthetic and natural analogs have been reported to possess a wide range of pharmacological activities like anti-inflammatory, anti-bacterial, anti-viral, anti-fungal, anti-leishmanial, anti-cancer, and anti-malarial, among others.<sup>2–6</sup> Some of the THIQ analogs that are used clinically are highlighted in Table 1.

To the best of our knowledge, there is a paucity of review articles for corroborating the biological significance of the THIQ analogs. Ysern *et al.* reviewed this class of compounds for the first time in the year 1981.<sup>7</sup> Scott *et al.* provided an in-depth analysis of the antitumor antibiotics,<sup>1</sup> whereas Singh *et al.* provided a patent review of THIQs in the field of therapeutics.<sup>8</sup> The present review, therefore, is aimed to provide a critical update on the biological activities of THIQ analogs along with their structure–activity relationship (SAR) in order to shed light on the impact of various functional groups that are responsible



*Prof. K. V. G. Chandra Sekhar completed his B. Pharm (Hons.), M. Pharm and Ph.D. in synthetic medicinal chemistry at BITS Pilani Rajasthan, India. Since 2015 he has been working as an associate professor at BITS Pilani Hyderabad campus. His areas of interest include medicinal chemistry and drug design. He successfully completed six research projects funded by UGC, DST and DBT, Govern-*

*ment of India. Currently Indo-Spain bilateral research is in progress in his lab. He has published over 50 research articles in well renowned international journals. He is an expert reviewer for various journals and has served as an examiner for Ph.D thesis at various universities.*



*Dr Selvaraj Kunjiappan is working as Assistant Professor of Biotechnology in the School of Bio and Chemical Engineering, Kalasalingam Academy of Research and Education, India. He received his PhD (Chemical Engineering) from Jadavpur University, Kolkata, India. His research interests are health care/pharmaceutically important lead compound design, synthesis and biomaterials isolated from environmentally dumped waste human hair, and waste biological materials like fish shells, and crab shells. The isolated biomaterial is applied to convert into nanoparticle nanocarriers for degenerative disease therapeutic formulations for overcoming multi drug resistance, targeted drug delivery and improved bioavailability.*

*Dr S. Murugesan is currently working as an Associate Professor in the Department of Pharmacy, BITS Pilani, Pilani Campus, Pilani, Rajasthan. In the year 2006, he enrolled in a Ph. D. program under the guidance of Dr Swastika Ganguly and acquired his doctorate in the year 2009 from Birla Institute of Technology, Mesra, Ranchi, India. Dr Murugesan is actively involved in research in computer-aided drug design and drug synthesis against HIV and allied opportunistic infections. He has more than 15 years of teaching and research experience. He has guided more than 30 B. Pharm, and 20 M. Pharm students for their dissertation work. Two scholars have already completed a full-time doctorate, while four are being pursued under his guidance. He has completed 3 research projects, including two as major projects from DST-SERB and DBT, India. Dr Murugesan has published more than 100 research papers in various peer-reviewed journals of international and national repute and presented more than 100 papers/posters in various international and national conferences.*



*Dr Subhash Chander is currently working as Assistant Professor II at Amity University Uttar Pradesh, Noida, India. He completed graduation in Pharmacy from GJU S & Tech, Hisar, in the year 2009, followed by a master's degree in Pharmaceutical Chemistry from NIPER, in the year 2011. He worked as Research Associate in a research organization for one and half years. He joined the research*

*group Dr S. Murugesan in 2012 at BITS, Pilani, and completed his PhD in the year 2017. Over the last decade, his team has been working on target specific drug discovery against HIV-1 and other allied opportunistic infections. He and his team have published more than 40 research and review articles, and two book chapters and filed two patents.*



*Dr S. Murugesan is currently working as an Associate Professor in the Department of Pharmacy, BITS Pilani, Pilani Campus, Pilani, Rajasthan. In the year 2006, he enrolled in a Ph. D. program under the guidance of Dr Swastika Ganguly and acquired his doctorate in the year 2009 from Birla Institute of Technology, Mesra, Ranchi, India. Dr Murugesan is actively involved in*

*research in computer-aided drug design and drug synthesis against HIV and allied opportunistic infections. He has more than 15 years of teaching and research experience. He has guided more than 30 B. Pharm, and 20 M. Pharm students for their dissertation work. Two scholars have already completed a full-time doctorate, while four are being pursued under his guidance. He has completed 3 research projects, including two as major projects from DST-SERB and DBT, India. Dr Murugesan has published more than 100 research papers in various peer-reviewed journals of international and national repute and presented more than 100 papers/posters in various international and national conferences.*



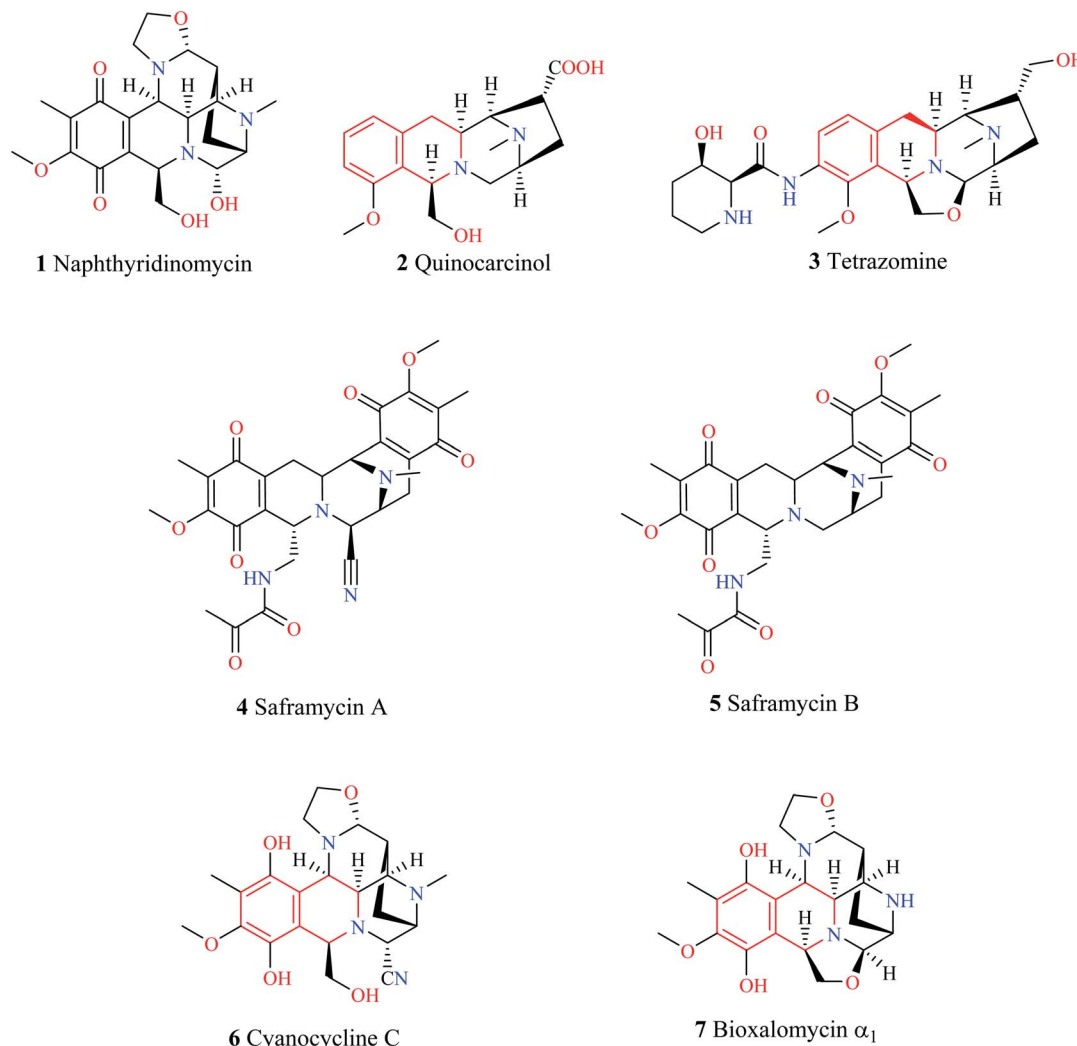


Fig. 1 THIQ containing antitumor antibiotics.

for dictating the desired activity. A note on the commonly used synthetic strategies for the construction of the THIQ core has also been discussed.

## 2. Strategies for synthesizing THIQ core

### 2.1 Pictet–Spengler condensation

Pictet–Spengler condensation is a commonly used reaction for the synthesis of heterocyclic scaffolds such as THIQ and tetrahydro  $\beta$ -carboline. The reaction was first described by Pictet and Spengler in the year 1911, wherein phenylethylamine **19** and dimethoxymethane in the presence of aq. HCl at 100 °C to afford THIQ **20** in 40% yield (Scheme 1).<sup>9</sup> Later, researchers have replaced dimethoxymethane with aldehydes to give one substituted THIQs.

A generalized mechanism (Scheme 2) consists of an initial condensation between a phenylethylamine derivative **21** and an aldehyde **22** to give an intermediate iminium **23**. The resulting imine is then activated using a Brønsted or Lewis acid, which

undergoes cyclization to give the one substituted THIQ product **24**.<sup>10</sup>

Different variants of Pictet–Spengler condensation are currently available which are currently used for the construction of racemic as well as asymmetric THIQ derivatives. One such variant of the Pictet–Spengler reaction for the synthesis of 1-substituted THIQ derivatives is shown in Scheme 3.<sup>11</sup> This reaction involved the synthesis of *N*-acetyl intermediate **26** from the starting material 2-(3,4-dimethoxyphenyl)-ethylamine **25**. Then intermediate compound **26** was converted into *N*-acylcarbamates **27**. The reduction of *N*-acylcarbamates **27** by diisobutyl aluminum hydride (DIBAL-H) followed by simultaneous cyclization mediated by  $\text{BF}_3 \cdot \text{OEt}_2$  leads to the titled compound **28**. The synthetic potential of this method was illustrated by the synthesis of tetrahydroisoquinoline alkaloids laudanosine **29**, xylopinine **30**, and isoindoloisoquinolone **31**.

Gremmen and co-workers reported the synthesis of enantiopure THIQs using a chiral auxiliary (1*R*,2*S*,5*R*)-(-) menthyl-*(S)*-*p*-toluene sulfinic acid (Andersen reagent).<sup>12</sup> This method (Scheme 4) involves the reaction of 2-(3,4-dimethoxyphenyl)-



Table 1 Clinically used drugs containing THIQ scaffold

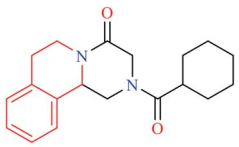
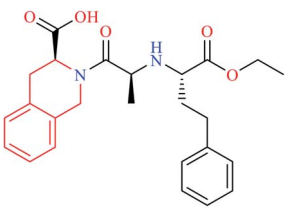
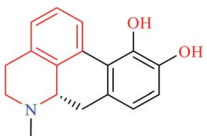
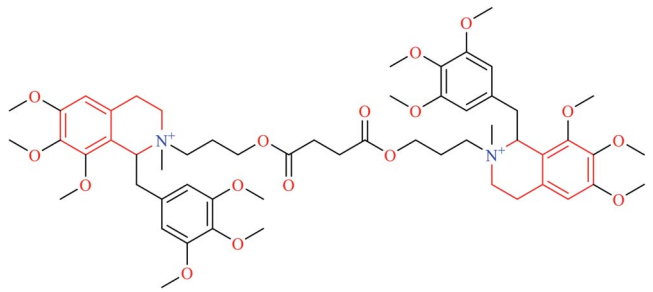
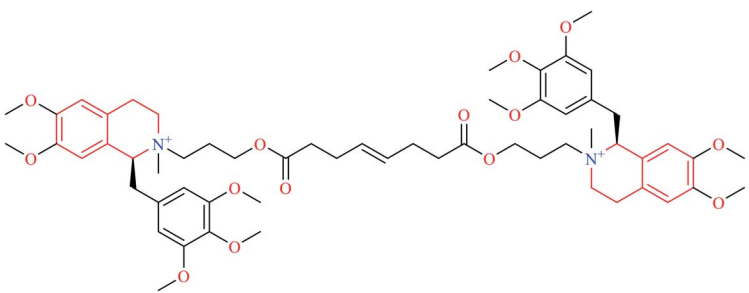
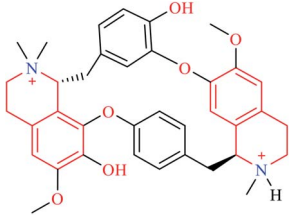
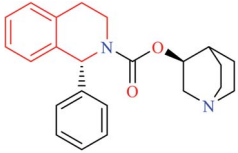
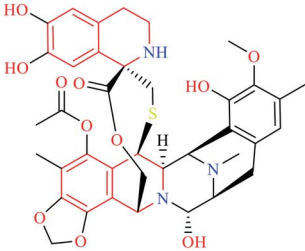
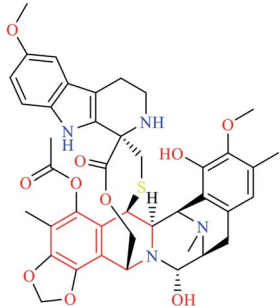
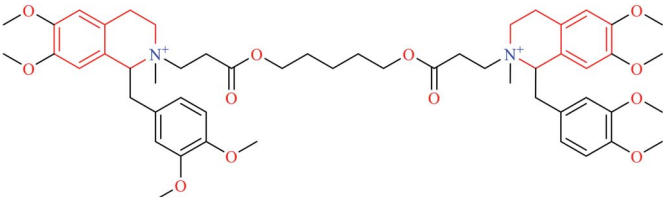
Name	Structure	Application
Praziquantel	 8	Anthelmintic
Quinapril	 9	Anti-hypertensive
Noscapine	 10	Anti-tussive
Apomorphine	 11	Anti-parkinsonian
Doxacurium	 12	Skeletal muscle relaxant
Mivacurium	 13	Skeletal muscle relaxant



Table 1 (Contd.)

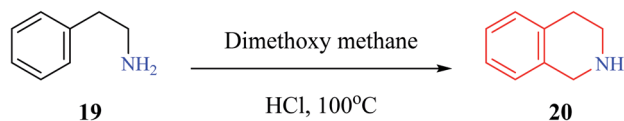
Name	Structure	Application
Tubocurarine	 14	Skeletal muscle relaxant
Solifenacin	 15	Used to treat overactive bladder
Trabectedin	 16	Anti-cancer
Lurbinectedin	 17	Anti-cancer
Atracurium	 18	Skeletal muscle relaxant

ethylamine **25** with *n*-butyllithium, followed by reaction with Andersen reagent **32** to give *N*-*p*-tolyl sulfinyl phenylethylamine **33**. The intermediate compound **33** then undergoes cyclization with different aldehydes *via* Pictet–Spengler condensation in the presence of  $\text{BF}_3 \cdot \text{OEt}_2$  to give the derivatives of THIQ **34**. The chiral auxiliary is then removed upon treating **34** with HCl in ethanol at 0 °C to give the final THIQ **35**. The synthetic potential

of this method was corroborated by the synthesis of THIQ natural product, (+) salsolidine **36**.

Mons *et al.* employed chiral catalysts (*R*)-TRIP **37** and (*S*)-BINOL **38** for the enantioselective synthesis of 1-substituted THIQs (Scheme 5).<sup>13</sup> The 2-(3-hydroxy-4-methoxy phenyl)-ethylamine **39** is first converted to intermediate compound **41** by reacting with *o*-nitrophenyl sulfonylchloride (NpsCl) **40**.





Scheme 1 THIQ synthesis by Pictet and Spengler.

Then, intermediate compound **41** undergoes asymmetric Pictet–Spengler reaction with different aldehydes to give the corresponding THIQs **42**. This methodology was employed for the synthesis of (*R*)-(+)-crispine A **46** (Scheme 6).

Microwave-assisted Pictet–Spengler reaction has also been used for the synthesis of 1-substituted THIQs.<sup>14</sup> In such a strategy (Scheme 7), cyclization of one representative compound 2-(3,4-dimethoxyphenyl) ethylamine **25** with benzaldehyde **47** in the presence of trifluoroacetic acid (TFA) under microwave irradiation for 15 minutes afforded the title compound **48** in 98% yield.

## 2.2 Bischler–Nepieralski reaction

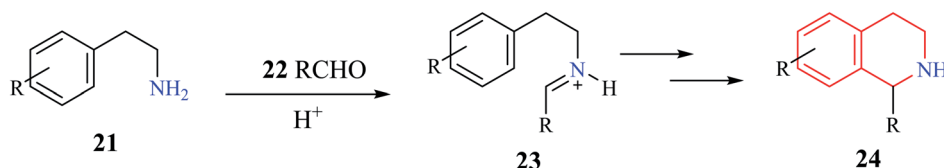
Bischler–Nepieralski reaction is another commonly used strategy for the synthesis of isoquinoline derivatives. The reaction involves the cyclization of an *N*-acyl derivative of  $\beta$ -phenylethylamine **49** in the presence of a dehydrating agent such as POCl<sub>3</sub>, P<sub>2</sub>O<sub>5</sub>, ZnCl<sub>2</sub> to generate 3,4-dihydro isoquinoline

derivatives **50** (Scheme 8). The resulting dihydro isoquinoline **50** is then reduced to THIQs **51** using reducing agents like sodium borohydride, sodium cyanoborohydride, or catalytic hydrogenation process. Mechanistically, the reaction is said to proceed *via* intramolecular electrophilic aromatic substitution reaction.<sup>15,16</sup> The presence of an electron-donating group like hydroxy or methoxy favors the cyclization step.

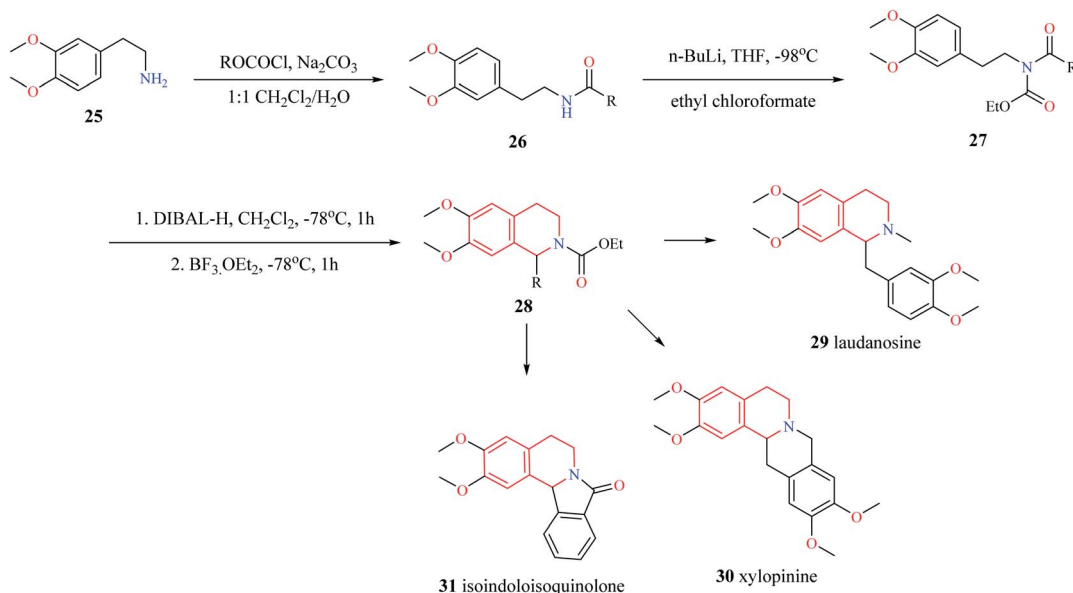
Mihoubi and co-workers synthesized THIQ derivatives **56–57** *via* Bischler–Nepieralski cyclization (Scheme 9).<sup>17</sup> Initially, compound **54** was obtained from vanillin **52** and nitropropane **53**. The compound **54** was then subjected to Bischler–Nepieralski cyclization using POCl<sub>3</sub> to give the dihydroisoquinoline moiety **55** which was then reduced using NaBH<sub>4</sub> to give the titled compounds **56–57**.

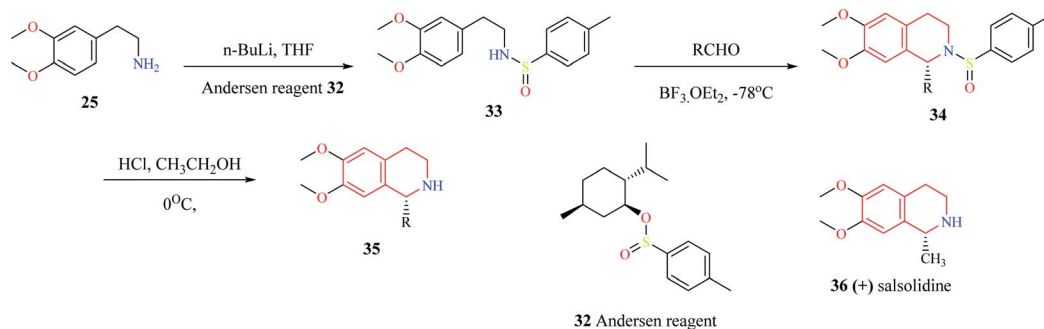
Mottinelli and co-workers synthesized *N*-substituted THIQs *via* Bischler–Nepieralski cyclization approach.<sup>18</sup> Initially, 3-methoxy-phenyl acetic acid **58** was converted to its amide **60**, which was then reduced to amine **61** using LiAlH<sub>4</sub>. The amine **61** was then converted to *N*-acyl derivative **62** using acyl chloride. Compound **62** was then subjected to Bischler–Nepieralski cyclization, followed by reduction with NaBH<sub>4</sub> to give the *N*-substituted titled THIQ derivative **63** (Scheme 10).

A biomimetic synthesis approach comprising of Bischler–Nepieralski cyclization and Noyori Asymmetric Transfer Hydrogenation (ATH) was used for the total synthesis of Dysoxylum alkaloids.<sup>19</sup> The total synthesis consists of 5 steps. The

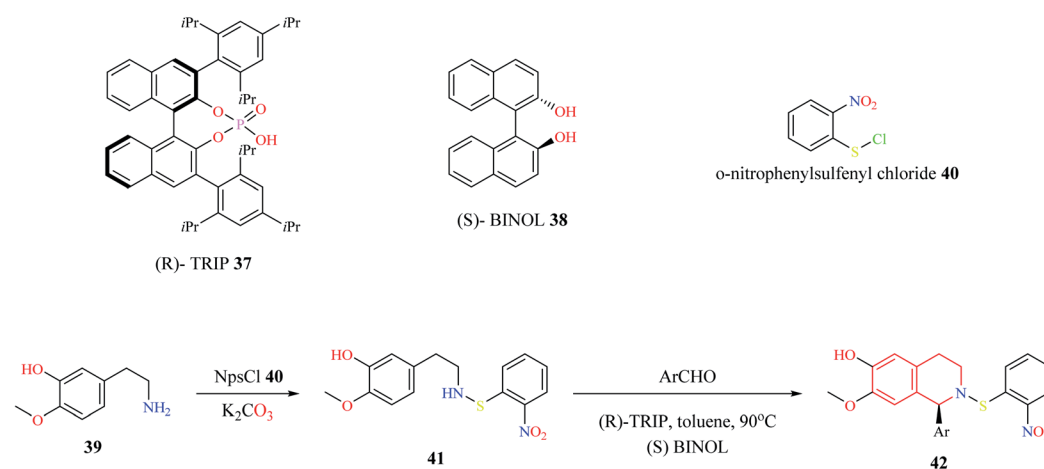


Scheme 2 Mechanism of Pictet–Spengler condensation.

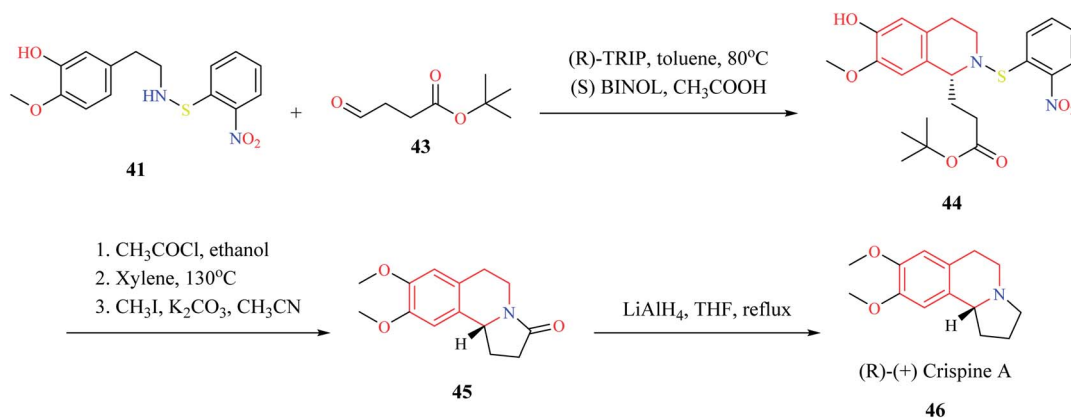
Scheme 3 Synthesis of compound **28**.



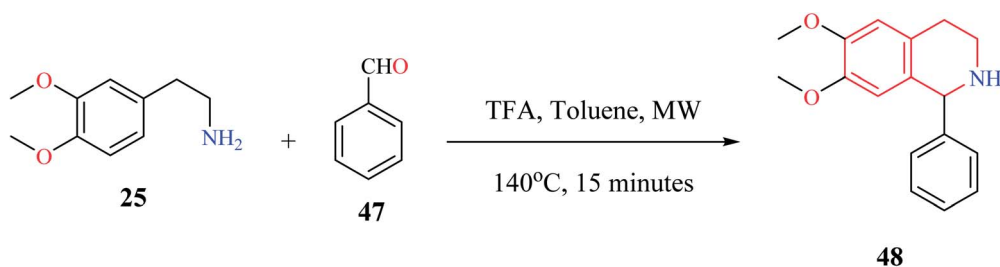
Scheme 4 Enantioselective synthesis of compound 35.



Scheme 5 Enantioselective synthesis of compound 42.

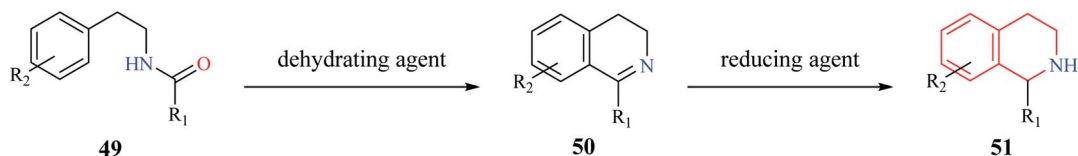


Scheme 6 Synthesis of (R)-(+)-crispine A 46.

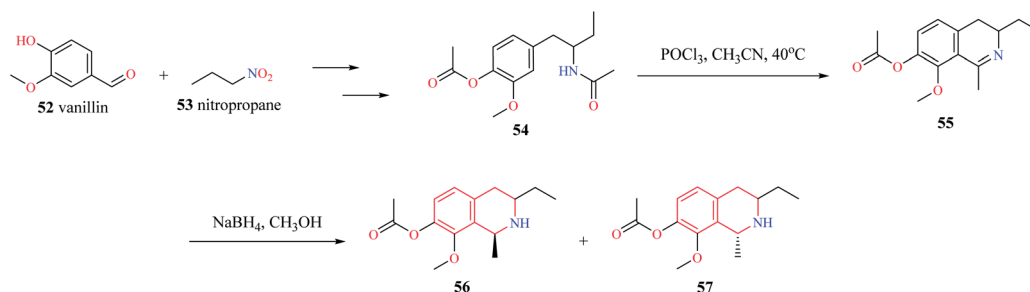


Scheme 7 Microwave-assisted synthesis of compound 48.





Scheme 8 Bischler–Nepieralski synthesis of THIQ.



Scheme 9 Synthesis of compounds 56–57.

first step involved the formation of zanthoxylamide protoalkaloid **66** from 2-(3,4-dimethoxyphenyl)-ethylamine **64** and (2)-3-phenylprop-2-enoic acid **65**. Intermediate compound **66** was then subjected to catalytic hydrogenation, which furnished second intermediate compound **67**. Intermediate compound **67** was then converted to the isoquinoline moiety **68** *via* Bischler–Nepieralski reaction. Compound **68** was then subjected to ATH reaction using a chiral catalyst (*R,R*)-RuTsDPEN **69** followed by reductive amination to obtain the final product **70** (Scheme 11). This approach was used for the total synthesis of Dysoxylum alkaloids **71a–i**.

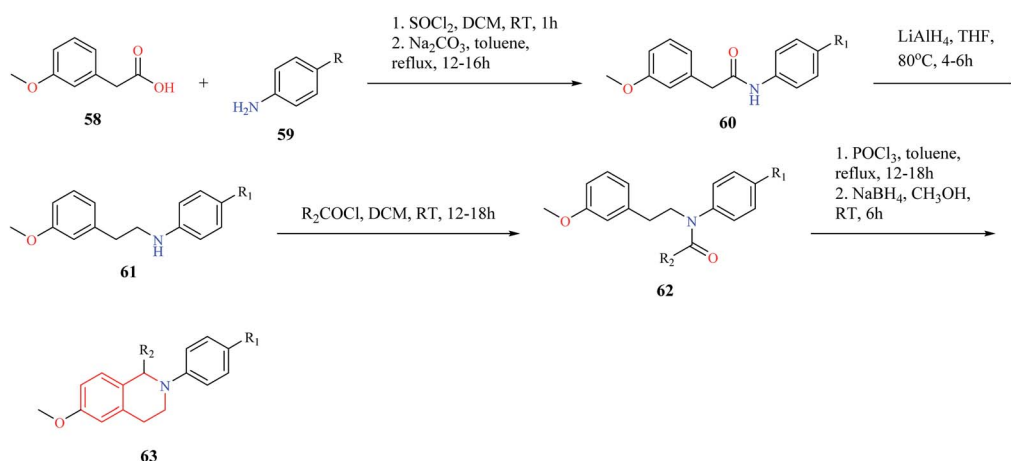
A similar synthetic approach comprising of Bischler–Nepieralski cyclization and Noyori ATH was used by Pieper and co-workers for the synthesis of enantioselective aporphine natural products **72–75** (Scheme 12).<sup>20</sup> The precursor compound **77** required for Bischler–Nepieralski cyclization was obtained from 3,4-disubstituted acetophenone **76** using

a sequence of reactions. Then intermediate compound **77** was treated with trifluoromethanesulfonic anhydride in the presence of 2-chloropyridine at low temperature to obtain the dihydro isoquinoline, which was then reduced using Noyori ATH to obtain the 1-substituted THIQ compound **78**. The THIQ compound **78** was then converted into the final compound **79**.

### 2.3 Multicomponent reactions (MCR)

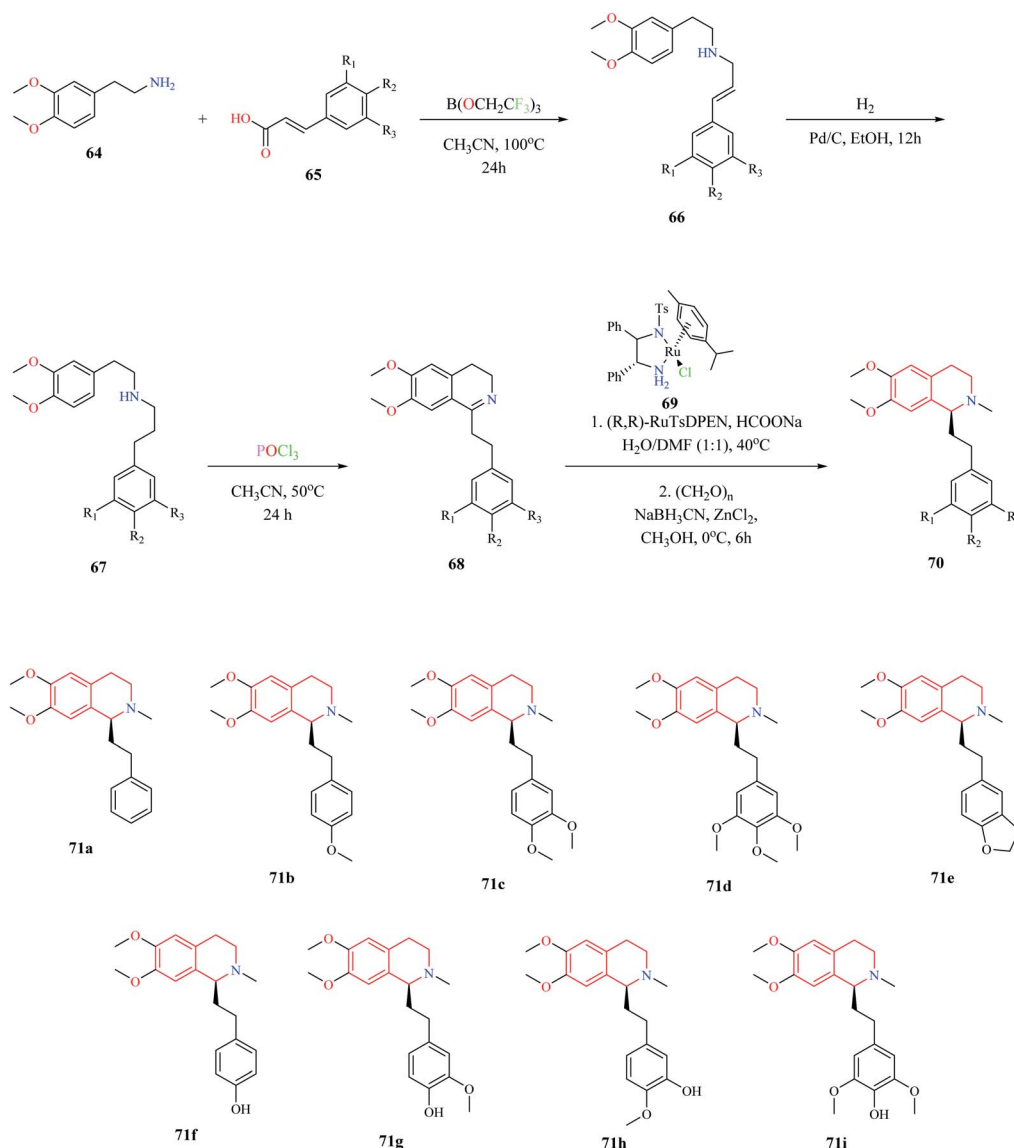
Multicomponent reactions (MCR) is a powerful strategy that has been routinely used for the construction of structurally diverse chemical compounds. MCR reactions have been used for the synthesis of compounds that have been bestowed with biological activity such as anticancer, antimicrobial, among others.<sup>21–23</sup>

Rong *et al.* utilized a MCR comprising of aromatic aldehydes **80**, *N*-methyl piperidin-4-one **81**, and malononitrile **82** for the synthesis



Scheme 10 Synthesis of compound 63.





Scheme 11 Biomimetic approach for the synthesis of Dysoxylum alkaloids.

of 6-amino-8-aryl-2-methyl-1,2,3,4-tetrahydroisoquinoline-5,7-dicarbonitriles **83** under solvent-free conditions (Scheme 13).<sup>24</sup> Almost 10 THIQ derivatives were synthesized with yields ranging from 85–97%.

A simple and efficient one-pot synthesis of novel *N*-alkyl substituted-6-amino-7-nitro-8-aryl-1,2,3,4-tetrahydroisoquinoline-5-carbonitrile derivatives **87** were synthesized using a MCR comprising of 1-alkylpiperidin-4-one **84**, malononitrile **85**, and  $\beta$ -nitro styrene **86** (Scheme 14).<sup>25</sup> The reactions were hypothesized to proceed sequentially *via* Knoevenagel condensation, Michael addition, Thorpe–Ziegler cyclization, and air-promoted dehydrogenation processes.

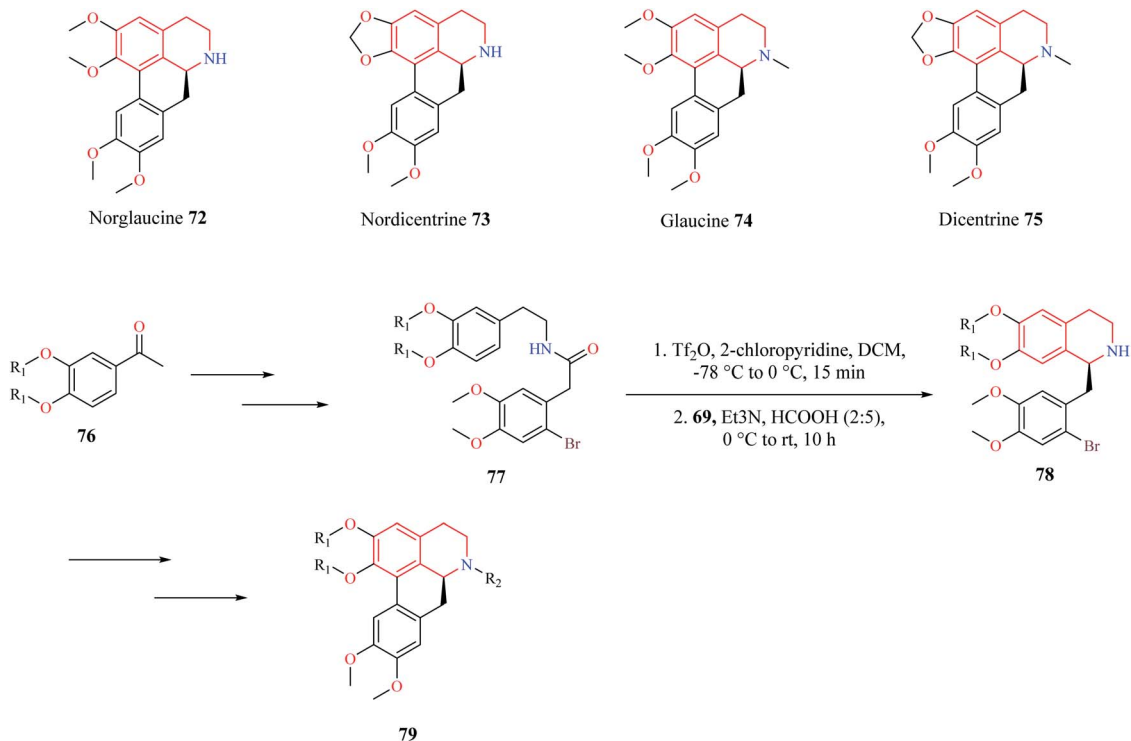
A one-pot, three-component synthesis comprising of 2-bromophenethylsulfonamide **88**, acryloyl chloride **89**, and primary or secondary amine **90** was used for the synthesis of functionalized THIQ derivatives **91** *via* domino Heck–aza-Michael reactions (Scheme 15).<sup>26</sup> Highly functionalized derivatives of THIQ

were synthesized using this domino reaction with moderate to excellent yields (28–97%).

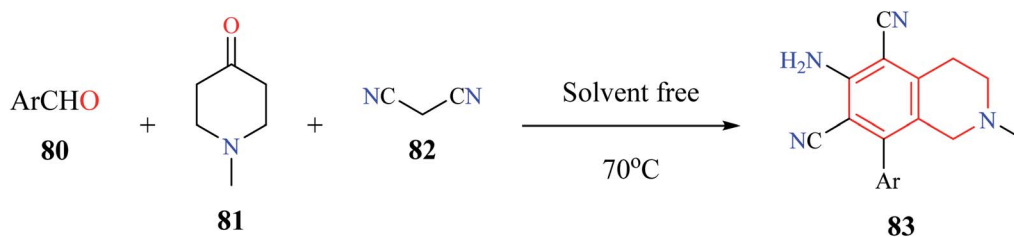
A one-pot, four-component (92–95) enantioselective synthesis of 1,3,4-substituted THIQ analogs **97** was reported by Jiang and co-workers (Scheme 16).<sup>27</sup> The cascade reaction comprising of Mannich–aza-Michael reaction was developed using a synergistic catalytic system consisting of ruthenium complex with a chiral Brønsted acid **96**. Almost 15 THIQ derivatives were synthesized using the optimized procedure with good yields and enantiomeric purity.

A one-pot, MCR comprising of 2-(2-bromoethyl)-benzaldehyde **98**, isocyanide **99**, amine **100**, and azide **101** was used for the synthesis of tetrazolyl-THIQ derivatives **102** under catalyst-free conditions (Scheme 17).<sup>28</sup> The optimized synthetic methodology exhibited a wide substrate scope with excellent yields (up to 99%). The reaction was postulated to proceed sequentially *via* an intramolecular cyclization/Ugi-azide reaction.





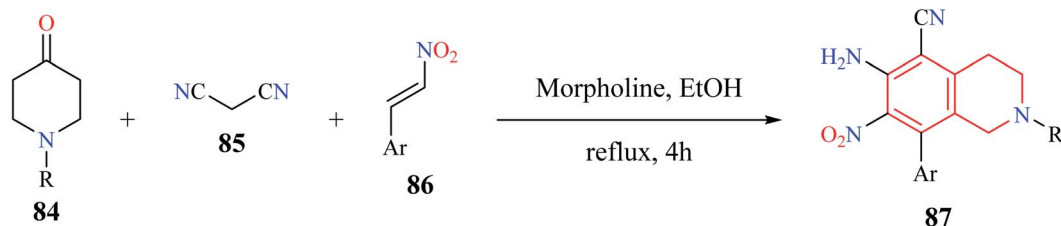
Scheme 12 Synthesis of aporphine natural products.

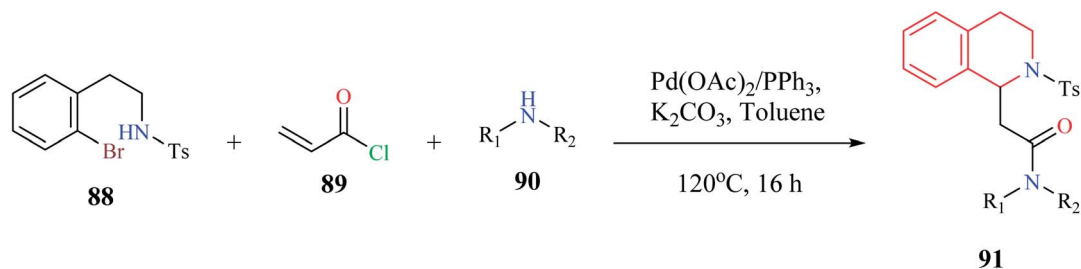
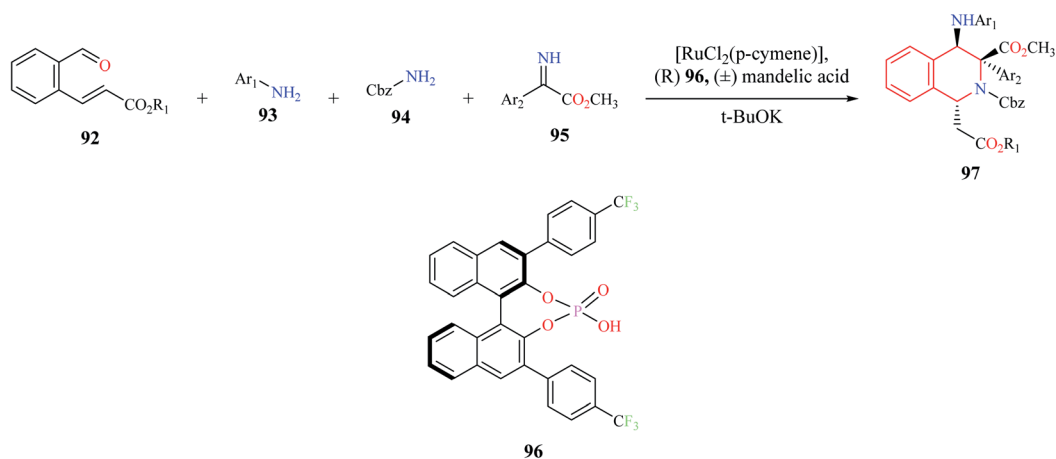
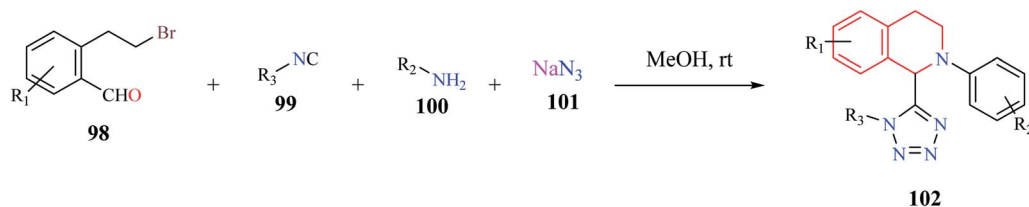
Scheme 13 Synthesis of compound **83**.

#### 2.4 Intramolecular hydroamination reaction

Henderson *et al.* reported the synthesis of THIQ derivatives *via* acid-catalyzed intramolecular hydroamination reaction from 2-aminoethyl styrene derivatives **103** which afforded good to excellent yields of the corresponding tetrahydroisoquinolines **104** (Scheme 18).<sup>29</sup> This approach represents an alternative strategy to the classical Pictet–Spengler method for the syntheses of THIQ compounds.

Different catalytic systems have been reported for the conversion of amino alkenes to corresponding THIQs *via* intramolecular hydroamination reaction. Ogata *et al.* reported the total synthesis of (*s*)-laudanosine which involved a key asymmetric intramolecular hydroamination reaction (Scheme 19).<sup>30</sup> The key intermediate **107** was obtained from 2-bromo-4,5-dimethoxy benzaldehyde **105** and 4-ethenyl-1,2-dimethoxy benzene **106** using a sequence of reactions. The intermediate compound **107** was then subjected to chiral bisoxazoline **108**–

Scheme 14 Synthesis of compound **87**.

Scheme 15 Synthesis of compound **91**.Scheme 16 Enantioselective synthesis of compound **97**.

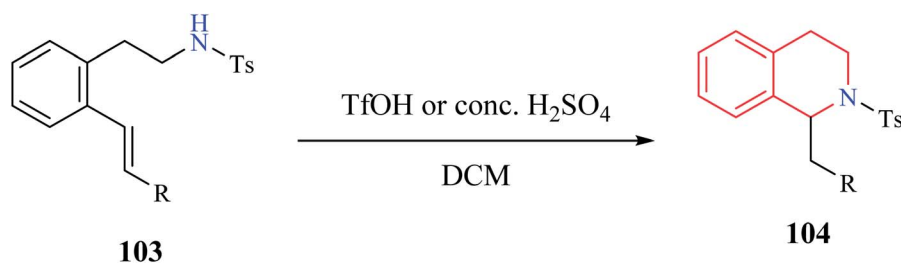
Scheme 17 Synthesis of tetrazolyl-THIQ analogs.

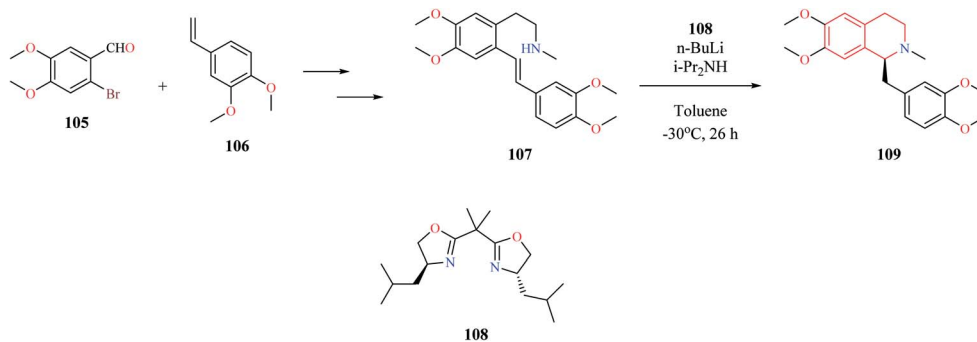
lithium diisopropylamide (LDA)-catalyzed asymmetric intramolecular hydroamination to obtain (*s*)-laudanidine **109**.

Tussing and co-workers reported a borane-catalyzed THIQ synthesis *via* intramolecular hydroamination (Scheme 20).<sup>31</sup> A sequential reaction comprising of tris-(pentafluorophenyl)-borane **110** catalyzed hydroamination and hydrogenation

reaction was used for the conversion of amino alkyne **111** to the corresponding THIQ compound **112** in 61% yield.

A convenient gold(III) chloride catalyzed intramolecular hydroamination for the synthesis of 1-alkyl-3-diethoxyphosphoryl-THIQ analog was reported by Murashkina and co-workers (Scheme 21).<sup>32</sup> Alkynyl substituted  $\alpha$ -

Scheme 18 Synthesis of compound **104**.



Scheme 19 Synthesis of (s)-laudanosine 109.

aminophosphonates **113** was first subjected to  $\text{AuCl}_3$  catalyzed hydroamination reaction, which was then followed by reduction with  $\text{NaBH}_4$  to give the THIQ analogs **114** with good to excellent yields.

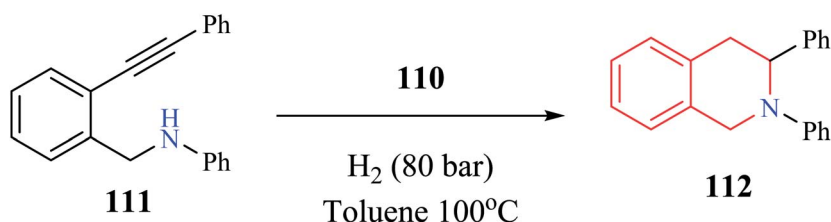
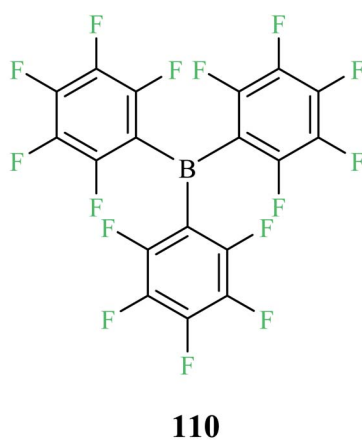
Dai and co-workers reported an enantioselective copper-catalyzed intramolecular hydroamination reaction for the preparation of THIQ analog (Scheme 22).<sup>33</sup> The amino alkene **115** was converted to enantiomerically pure compound **117** with the aid of  $\text{Cu}(\text{OAc})_2$  and a chiral catalyst (*R,R*)-Ph-BPE **116**.

Pictet–Spengler condensation and Bischler–Nepieralski reaction are some of the routinely used synthetic strategies for the construction of THIQ core. However, they often involve multiple steps and are restricted to substitution at the 1<sup>st</sup> position of the THIQ nucleus. On the other hand, MCR provides an exciting opportunity to generate diverse libraries of THIQs in one-pot and atom economic synthetic protocols.

## 3. Biological activity

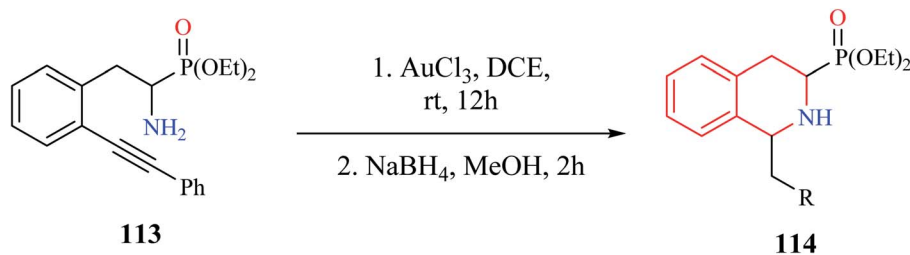
### 3.1 Anti-bacterial activity

Guzman *et al.* synthesized three series (A, B, C) of THIQ analogs to elucidate a common anti-TB pharmacophore.<sup>34</sup> The synthesized analogs were evaluated against two mycobacterium species – *Mycobacterium bovis* BCG and *M. tuberculosis* H<sub>37</sub>Rv. Most of the compounds in the A-series were found to be inactive except compound **118** which exhibited moderate potency against both the mycobacterium species. Compounds **119** and **120** were found to be the most potent from the B series. The third series of compounds were designed and synthesized based on the structure of active compound **120**. **121–123** were some of the compounds that were found to be active in this series. Moreover, the active compounds from each of the three series were evaluated for the inhibitory property against MurE

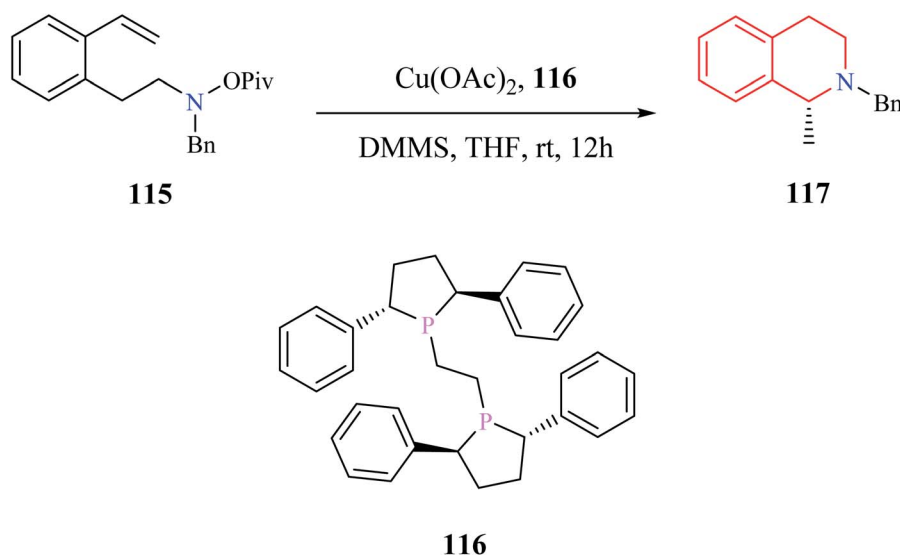


Scheme 20 Borane-catalyzed intramolecular hydroamination reaction for the synthesis of compound 112.





Scheme 21 Gold catalyzed intramolecular hydroamination reaction for the synthesis of compound 114.



Scheme 22 Enantioselective copper-catalyzed intramolecular hydroamination reaction for the synthesis of compound 117.

synthetase, a crucial enzyme in peptidoglycan biosynthesis. Compounds **119**, **120**, **122** exhibited effective MurE inhibition. However, the correlation between the MurE inhibition and phenotypic inhibitory effects was low, indicating another possible mechanism of action. The SAR is discussed in Fig. 2.

Farha *et al.* designed and synthesized analogs of ticlopidine **125** and clopidogrel **126** (Fig. 3), anti-platelet drugs used for cardiac disorders.<sup>35</sup> Anti-platelet drugs ticlopidine and clopidogrel have been shown to potentiate the activity of beta-lactam antibiotics against methicillin-resistant *Staphylococcus aureus* (MRSA) by inhibiting TarO, the first enzyme in the synthesis of wall teichoic acids (WTA). Ticlopidine being a prodrug is extensively metabolized to its anti-platelet metabolite leaving only traces of the intact drug in the plasma. Hence, the thiophene ring of ticlopidine as well as its analog clopidogrel was replaced with a phenyl ring to generate compounds **127** and **128** containing the THIQ nucleus. Several derivatives were designed and synthesized based on compounds **127** and **128** and they were evaluated for their synergism with cefuroxime against MRSA. Compound **129** exhibited maximum synergism with cefuroxime.

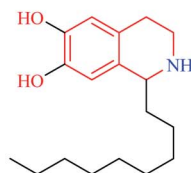
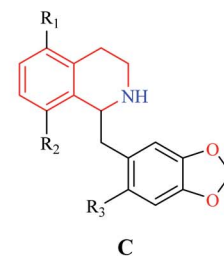
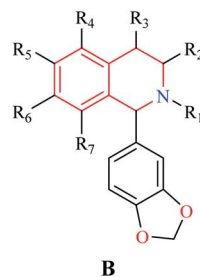
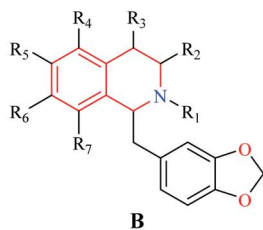
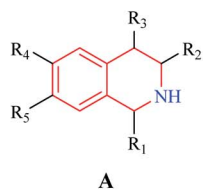
A novel compound (*E*)-2-benzyl-3-(furan-3-yl)-6,7-dimethoxy-4-(2-phenyl-1*H*-indene-1-ylidene)-1,2,3,4-tetrahydroisoquinoline **131** (Fig. 4) was synthesized and evaluated for its antibacterial property against eight pathogenic bacterial strains.<sup>36</sup> The strains that were

most susceptible to the action of compound **131** at 25 µg ml<sup>-1</sup> were *Staphylococcus epidermidis* and *Klebsiella pneumonia*.

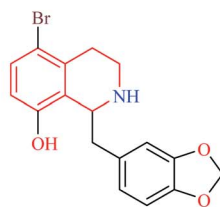
Novel derivatives of THIQ: chiral quaternary *N*-spiro ammonium bromides containing 3',4'-dihydro-1'*H*-spiro[isoinoline-2,2'-isoquinoline] were evaluated for their bacteriostatic and bactericidal property against nine pathogenic bacterial strains.<sup>37</sup> Most of the analogs were more potent against Gram-negative bacterial strains. Compounds **132**–**135** (Fig. 5) were found to be more potent than control norfloxacin against *Campylobacter jejuni*. Compound **136** was the most promising compound as it possessed more potent antibacterial property than ciprofloxacin against *Streptococcus mutans* and *Bacillus subtilis*.

Novel THIQ analogs containing lipid-like choline moiety were synthesized and evaluated for their antibacterial properties by Zablotskaya *et al.* Incorporation of these lipid-like substituents may improve the absorption properties of the compounds. Compounds **138** and **139** (Fig. 6) were some of the analogs that exhibited good antibacterial activity. Compound **138** was more active against Gram-positive bacteria's whereas compound **139** was superior against Gram-negative bacterial species. Moreover, these compounds also possessed inhibitory property against DNA gyrase, a vital enzyme that is involved in DNA topology.<sup>38</sup> Similarly, organosilicon lipid-like derivatives of THIQ analogs were also reported by Zablotskaya *et al.*

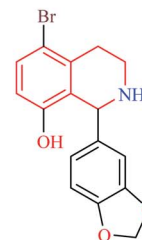




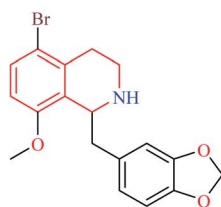
MIC= 80  $\mu\text{g/ml}$  against *M. bovis*  
60  $\mu\text{g/ml}$  against *M. tuberculosis*  
IC<sub>50</sub>= 186  $\mu\text{M}$  against MurE



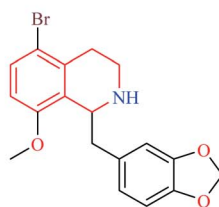
MIC= 20  $\mu\text{g/ml}$  against *M. bovis*  
IC<sub>50</sub>= <111  $\mu\text{M}$  against MurE



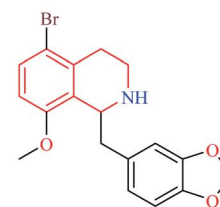
MIC= 60  $\mu\text{g/ml}$  against *M. bovis*  
IC<sub>50</sub>= <111  $\mu\text{M}$  against MurE



MIC= 20  $\mu\text{g/ml}$  against *M. bovis*  
40  $\mu\text{g/ml}$  against *M. tuberculosis*  
IC<sub>50</sub>= 165  $\mu\text{M}$  against MurE

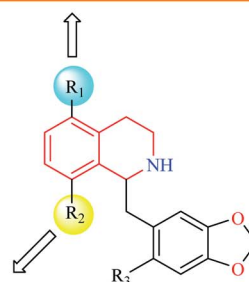


MIC= 50  $\mu\text{g/ml}$  against *M. bovis*  
30  $\mu\text{g/ml}$  against *M. tuberculosis*  
IC<sub>50</sub>= <111  $\mu\text{M}$  against MurE



MIC= 40  $\mu\text{g/ml}$  against *M. bovis*  
40  $\mu\text{g/ml}$  against *M. tuberculosis*

Halogens are important for activity and MurE inhibition.  
Br is preferred over Cl and I.



Hydroxy group is preferred.  
Substitution of methoxy groups leads to cytotoxicity

**124**

Fig. 2 THIQ analogs 118–123 as anti-bacterial agents.

Compounds 140 and 141 were found to exhibit good antibacterial activity along with DNA gyrase inhibitory action.<sup>39</sup>

A series of 5,8-disubstituted THIQ analogs were synthesized by Lu *et al.* The synthesized analogs were evaluated for their

anti-mycobacterial property.<sup>40</sup> Compounds 142 and 143 (Fig. 7) were some of the potent analogs against *Mycobacterium tuberculosis*. Compound 143 also exhibited good clearance property. Moreover, it was also found to exhibit potent inhibitory activity



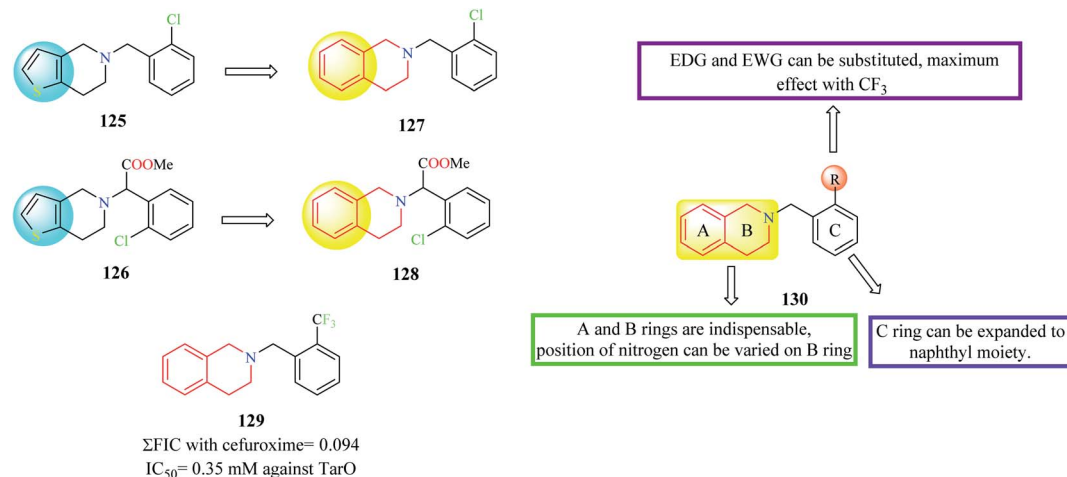
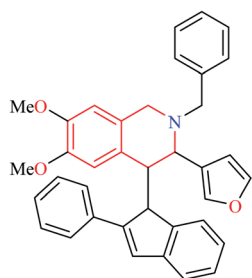


Fig. 3 SAR profile of ticlopidine and clopidogrel analogs.



131

Zone of inhibition (ZOI) = 22 mm against *S. epidermis*  
20 mm against *K. pneumonia*

Fig. 4 Structure of compound 131.

against mycobacterial (*M. smegmatis*) ATP synthetase enzyme with an IC<sub>50</sub> value of 1.8 μg ml<sup>-1</sup> with about 9-fold selectivity over the human counterpart. The SAR of these groups of analogs is summarized in Fig. 7.

### 3.2 Anti-fungal activity

Novel *N*-substituted THIQ analogs were synthesized and evaluated for their antifungal activity.<sup>41</sup> Initially, these analogs were evaluated against four fungi species and their zone of inhibition was determined. Compounds **145** and **146** (Fig. 8) produced a comparable zone of inhibition against *Candida glabrata* as that of the standard drug clotrimazole. Their MIC values were determined against different fungal species. Compound **145** exhibited the most potent activity against *Saccharomyces cerevisiae* (MIC = 1 μg ml<sup>-1</sup>) whereas compound **146** was more potent against *Yarrowia lipolytica* with a MIC value of 2.5 μg ml<sup>-1</sup>. Furthermore, these compounds were shown to interfere with the ergosterol biosynthetic pathway. Specifically, these compounds inhibited delta-8,7-isomerase.

The antifungal potency of novel analogs of the pyrrolo-THIQ fused system was reported by Sutariya and co-workers.<sup>42</sup> Compound **148** and its stereoisomer compound **149** (Fig. 9)

exhibited equipotent activity as that of nystatin against pathogenic fungi *C. albicans*. Two bis (THIQ) derivatives of undecane **150** and **151** were evaluated for their antifungal activity against *C. albicans*.<sup>43</sup> Compound **150** (zone of inhibition = 20 mm) exhibited better antifungal activity than nystatin (zone of inhibition = 15 mm). Zablotskaya and co-workers also evaluated compounds **138–141** for their antifungal property.<sup>38,39</sup> They exhibited potent antifungal activity as that of the standard drug fluconazole.

### 3.3 Anti-viral activity

Murugesan *et al.* synthesized novel THIQ analogs and evaluated their Human immunodeficiency virus-1 (HIV-1) reverse transcriptase (RT) inhibitory property.<sup>44</sup> Compounds **152** and **153** exhibited moderate activity against HIV-1 RT. Molecular docking studies were performed to predict the binding pose of compounds **152** and **153** (Fig. 10). Docking studies indicated that these compounds adopted “butterfly-like” conformation like non-nucleoside reverse transcriptase inhibitors (NNRTIs) (*e.g.* nevirapine, efavirenz) within the binding pocket of RT. Three novel derivatives of THIQ analogs **154–156** as NNRTIs were shown to exhibit potent activity against the HIV RT.<sup>45</sup> Both these analogs inhibited the polymerase activity of the RT in the nanomolar range. The interactions of compound **156** in the binding pocket of the RT are depicted in Fig. 11. Moreover, both the compounds also prevented HIV-induced cell death *in vitro*. Continuing their studies on identifying potent anti-HIV derivatives, Zhan and others synthesized 2-(3-(2-chlorophenyl)pyrazin-2-ylthio)-*N*-arylacetamide analogs *via* a structure-based bioisosterism approach and evaluated their anti-HIV activity.<sup>46</sup> One of the derivatives **157** containing THIQ scaffold exhibited potent anti-HIV activity (IC<sub>50</sub> = 4.10 μm).

Chander *et al.* designed and synthesized two series of THIQ analogs **158** and **159** (Fig. 12) as HIV-RT inhibitors.<sup>48</sup> Thirty derivatives were synthesized based on compounds **158** and **159** and about eight analogs exhibited more than 50% inhibition at 100 μM. Compounds **160** and **61** were the most promising of them all with % RT inhibition values of 74.82% and 72.58%



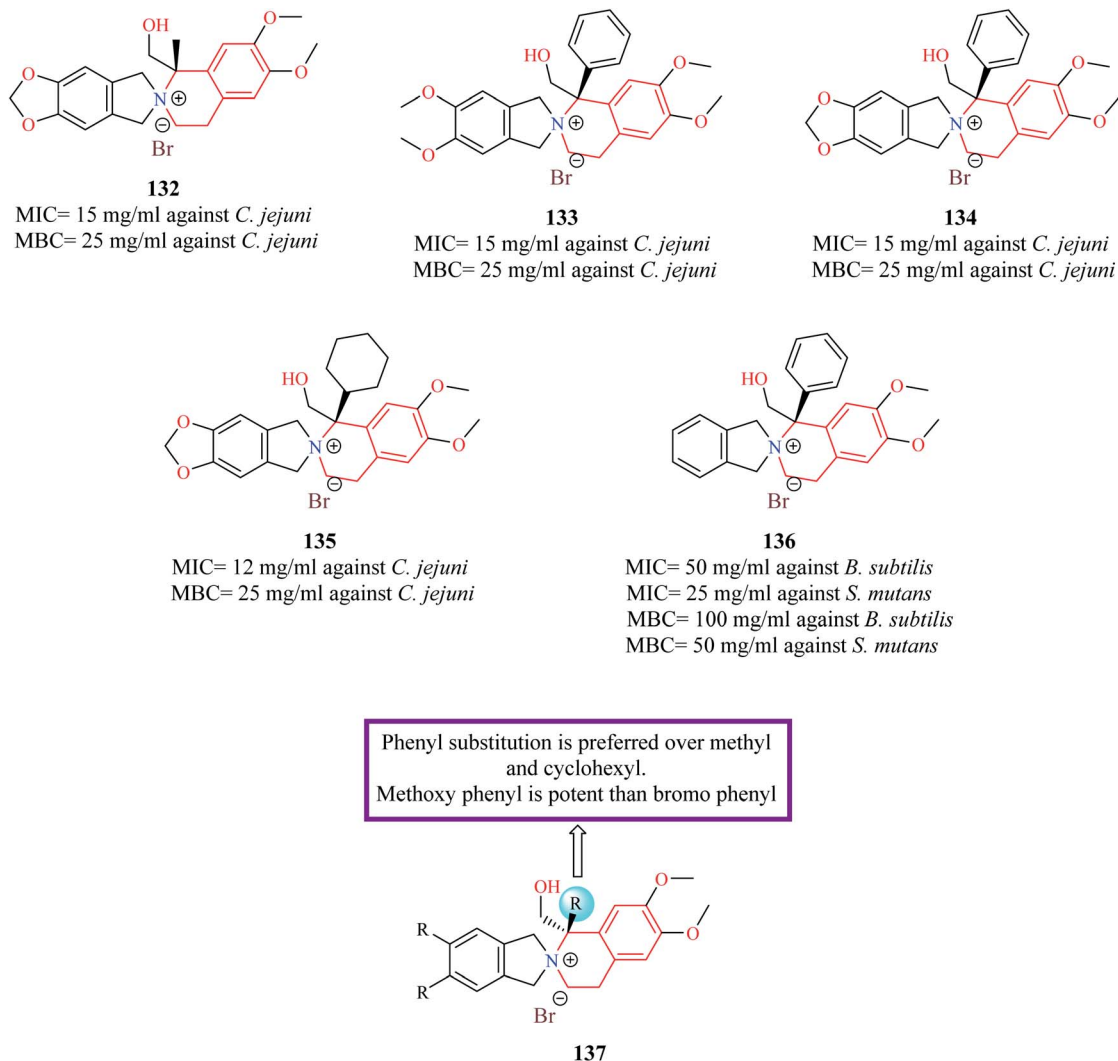


Fig. 5 Structure of THIQ analogs 132–136 as anti-bacterial agents.

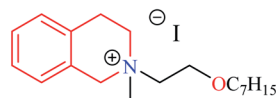
respectively. Molecular docking studies were also performed to shed light on the binding pattern of compounds **160** and **161** at the active site of the target HIV-1 RT. 6,7-Dimethoxy THIQ of both the analogs were found to exhibit hydrophobic contacts with Tyr-188, Tyr-181, and Trp-229. The nitrogen of acetamide exhibited hydrogen bond interaction with Lys-101, an active residue of RT. These interactions may be the reason for their significant *in vitro* activity.

Compound **164** (BMS-626529) (Fig. 13) is a potent HIV-1 attachment inhibitor. The prodrug form of compound **164**, Fostemsavir **165** is FDA approved for the treatment of HIV. The benzamide moiety in the compound **164** was susceptible to *in vivo* metabolism. Therefore, Swiderski and co-workers made efforts to replace the piperazine benzamide moiety with THIQ scaffold in order to improve the metabolic stability and solubility to preclude the use of prodrug.<sup>6</sup> Initial efforts lead to the development of compounds **166** and **167** with enhanced potency against HIV-1 when compared with compound **164**. Compound **166** also exhibited similar solubility ( $19 \mu\text{g ml}^{-1}$ ) like that of compound **164** ( $22 \mu\text{g ml}^{-1}$ ). However, compounds

**166** and **167** had a very low metabolic stability when compared with compound **164**. Various analogs were synthesized based on compound **167** in order to improve the metabolic stability without comprising solubility. Though the potency of compounds was found to increase, none of the synthesized analogs were found to exhibit better properties than compound **167**. Further studies identified 1<sup>st</sup> position of the THIQ scaffold as a soft spot for metabolism. The 1<sup>st</sup> position of the THIQ in compound **167** was then functionalized to generate compounds **168** and **169**. The potency of both the compounds decreased when compared with compound **167**. Moreover, aqueous solubility decreased, and cytotoxicity enhanced. This study demonstrates the immense potential of the THIQ scaffold against HIV.

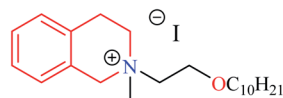
PA<sub>N</sub> (N-terminus of polymeric acidic protein) endonuclease is considered an ideal target for the development of anti-influenza agents. They are highly conserved across different influenza strains and more importantly, have no human counterpart. Liao *et al.* modified dopamine **170** (Fig. 14) to develop novel THIQ analogs.<sup>49</sup> Compounds **171** and **172** exhibited potent activity against influenza virus *A in vitro*. Compound **172**





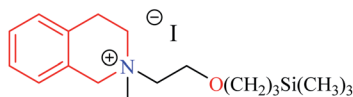
138

MIC = 1  $\mu\text{g/ml}$  against *Staphylococcus aureus*  
 = 2  $\mu\text{g/ml}$  against *Bacillus cereus*  
 = 128  $\mu\text{g/ml}$  against *Escherichia coli*  
 = 128  $\mu\text{g/ml}$  against *Pseudomonas aeruginosa*



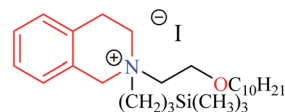
139

MIC = 2  $\mu\text{g/ml}$  against *Staphylococcus aureus*  
 = 4  $\mu\text{g/ml}$  against *Bacillus cereus*  
 = 64  $\mu\text{g/ml}$  against *Escherichia coli*  
 = 64  $\mu\text{g/ml}$  against *Pseudomonas aeruginosa*  
 = 64  $\mu\text{g/ml}$  against *Proteus mirabilis*



140

MIC = 4  $\mu\text{g/ml}$  against *Staphylococcus aureus*  
 = 8  $\mu\text{g/ml}$  against *Bacillus cereus*  
 = 64  $\mu\text{g/ml}$  against *Escherichia coli*  
 = 128  $\mu\text{g/ml}$  against *Pseudomonas aeruginosa*  
 = 256  $\mu\text{g/ml}$  against *Proteus mirabilis*



141

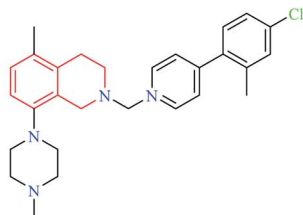
MIC = 0.5  $\mu\text{g/ml}$  against *Staphylococcus aureus*  
 = 4  $\mu\text{g/ml}$  against *Bacillus cereus*  
 = 64  $\mu\text{g/ml}$  against *Escherichia coli*

Fig. 6 Structure of compounds 138–141 as anti-bacterial agents.

exhibited concentration-dependent inhibition of  $\text{PA}_N$  endonuclease with an  $\text{EC}_{50}$  value of 489.39 nM and a  $K_D$  value of 94.19 nM. Molecular docking studies revealed that compound 172 was able to occupy the active site in the target protein. Compound 172 was able to form hydrophobic contacts with the active site residue His 41 as well as chelate the Mn metal ion in the active site.

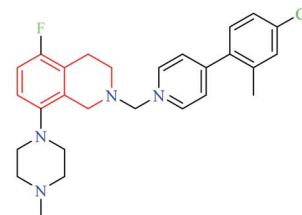
### 3.4 Anti-malarial activity

High-throughput phenotypic screening of over 300 000 compounds was performed against the 3D7 strain of *Plasmodium falciparum* to discover novel hits for pre-clinical development.<sup>50</sup> Phenotypic screening resulted in the identification of about 1300 validated hits. Most of the potent hits belonged to three different scaffolds: THIQ, diamionaphthoquinones, and



142

$\text{MIC}_{90}$  = 0.79  $\mu\text{g/ml}$  against *Mycobacterium tuberculosis*



143

$\text{MIC}_{90}$  = 1.2  $\mu\text{g/ml}$  against *Mycobacterium tuberculosis*

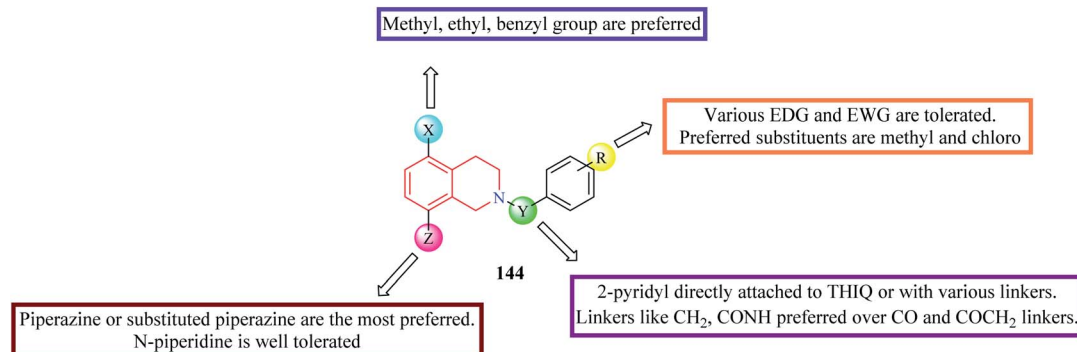
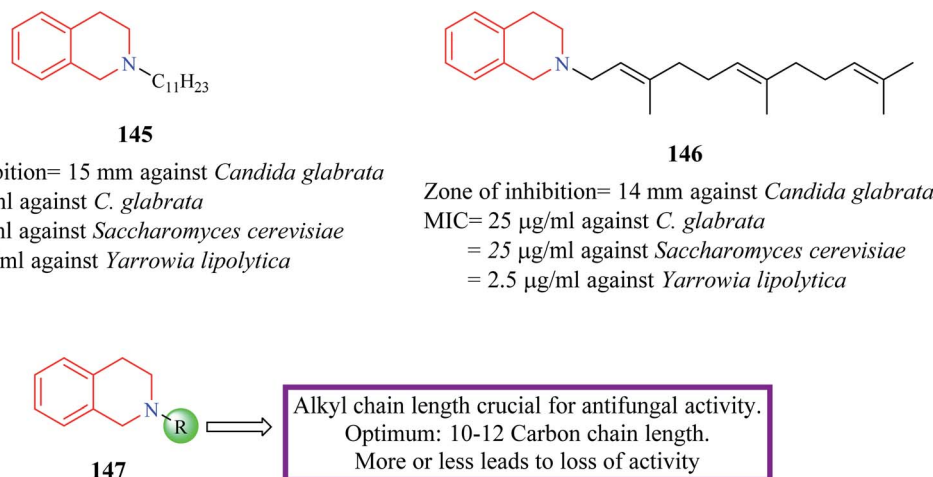


Fig. 7 SAR profile of 5,8-disubstituted THIQ analogs.



Fig. 8 SAR profile of *N*-substituted THIQ analogs along with their anti-fungal activity.

dihydropyridine. Over 40 analogs belonged to the THIQ core with most of the compounds exhibiting potent activity against drug-resistant strains of malaria. Compound **173** (Fig. 15) was identified as the most active of them all with  $\text{EC}_{50}$  in the sub-nanomolar range against all the tested malarial strains. Compound **173** also exhibited acceptable pharmacokinetic properties.<sup>50</sup> However, the compounds were found to exhibit poor solubility and metabolic vulnerability. Further hit-to-lead studies were conducted on compound **173** to generate pre-clinical candidates for development.<sup>51</sup> Different groups were substituted on *N*-2, *C*-3, and *C*-4 positions of compound **173** to address potency, solubility, and metabolic stability. Phenyl group was the most preferred substituent on the amide nitrogen. Substitution of aliphatic or other aromatic systems did not improve the potency. In general, EDG groups were

preferred on the *para* position (the only exception being fluoro), and EWG groups were preferred on the *meta*-position in the phenyl ring. However, none of the substituents improved solubility. Hence, different substitutions were made on *C*-3 to address this problem. Although potency improved with a 5-membered heterocyclic ring system, no improvement in solubility was observed. A consensus was obtained with pyridine or pyrazole substitution. There was a slight decrease in potency upon pyridine substitution, but solubility was enhanced. The next substitution on *N*-2 was done to address the problem related to metabolic vulnerability as well as solubility. Both the lipophilicity as well as the shape of the substituent on *N*-2 had a profound effect on the potency. Though better potency was observed with iso-butyl substitution, they are metabolically labile. Therefore, *N*-2,2,2-trifluoroethyl substituent was

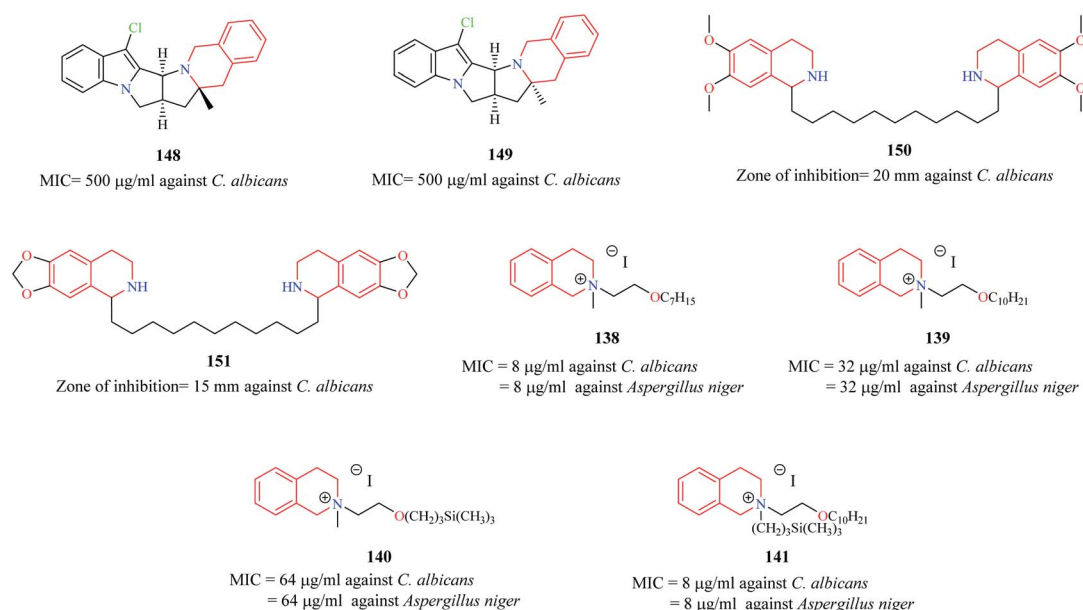


Fig. 9 Structure of anti-fungal THIQ analogs 148–151.



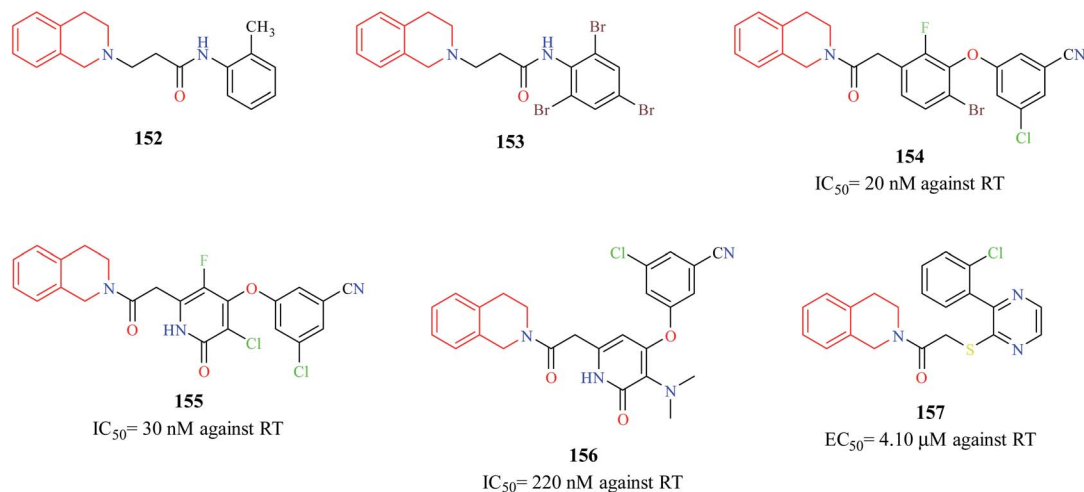


Fig. 10 Structure of THIQ analogs 152–157 as NNRTIs.

substituted to afford stability. After extensive studies, two compounds 174 and 175 (also known as (+)-SJ733) were identified as ideal lead candidates.<sup>51</sup> Both the compounds exhibited good solubility and metabolic stability, and potent antimalarial activity *in vitro* and *in vivo*. Compound 175 was then subjected to intense pre-clinical studies.<sup>52</sup> The studies demonstrated that compound 175 possessed potent *in vivo* activity, high oral bioavailability, and good safety margins. Further, mechanistic studies indicated that compound 175 exhibits its antimalarial activity by inhibiting *Plasmodium falciparum* ATPase 4 (PfATP4).<sup>52</sup> Compound 175 was also shown to have a favorable pharmacokinetic and safety profile in phase 1 clinical trials in humans.<sup>53</sup>

21 novel derivatives of 1-aryl-6-hydroxy-THIQ analogs were designed and synthesized by Hanna *et al.*<sup>54</sup> The synthesized analogs were evaluated for their antiplasmodial activity against *P. falciparum*. More than 15 compounds were found to exhibit moderate antimalarial activity. Compounds 177–179 (Fig. 16) exhibited potent antimalarial activity comparable to that of the

standard drug chloroquine. They also possessed good selectivity indices and were also predicted to possess good pharmacokinetic properties. Further mechanistic and *in vivo* studies are required to further their stance as prospective antimalarial drug candidates.

Three THIQ analogs 181–183 (Fig. 17) from Medicines for Malaria Venture (MMV) Malaria Box were assessed for their antiplasmodial activity against *P. falciparum* in different stages of its life cycle: asexual blood stages, mature gametocyte stages, and early sporogonic stages.<sup>55</sup> All three THIQ analogs exhibited potent activity against the asexual blood stage of *P. falciparum*. They were also highly potent against chloroquine-resistant *P. falciparum* W2 strain with IC<sub>50</sub> values between 0.070–0.133 μM. They also exhibited good *P. falciparum* gametocidal activity. They were also found to have a profound effect on the early sporogonic stage.

### 3.5 Anti-leishmanial activity

Chauhan *et al.* synthesized a series of triazine dimers as potential antileishmanial agents.<sup>56</sup> Triazine-THIQ hybrid 184

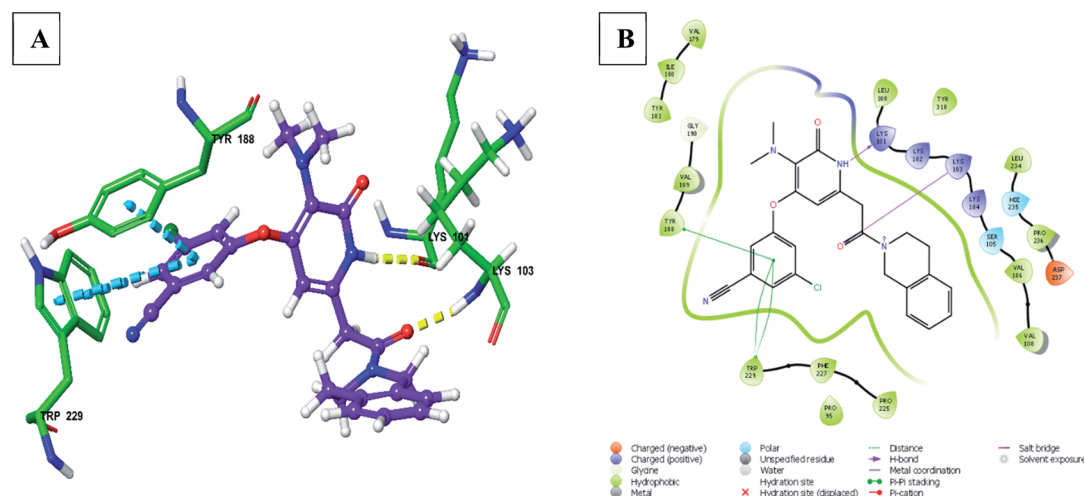


Fig. 11 (A) 3D docked pose of compound 156 in the binding pocket of RT (yellow – hydrogen bond, blue –  $\pi$ - $\pi$  interaction), (B) interaction of compound 156 with surrounding amino acid residues in 2D (PDB ID – 3FFI) (visualized using Maestro visualizer).<sup>47</sup>



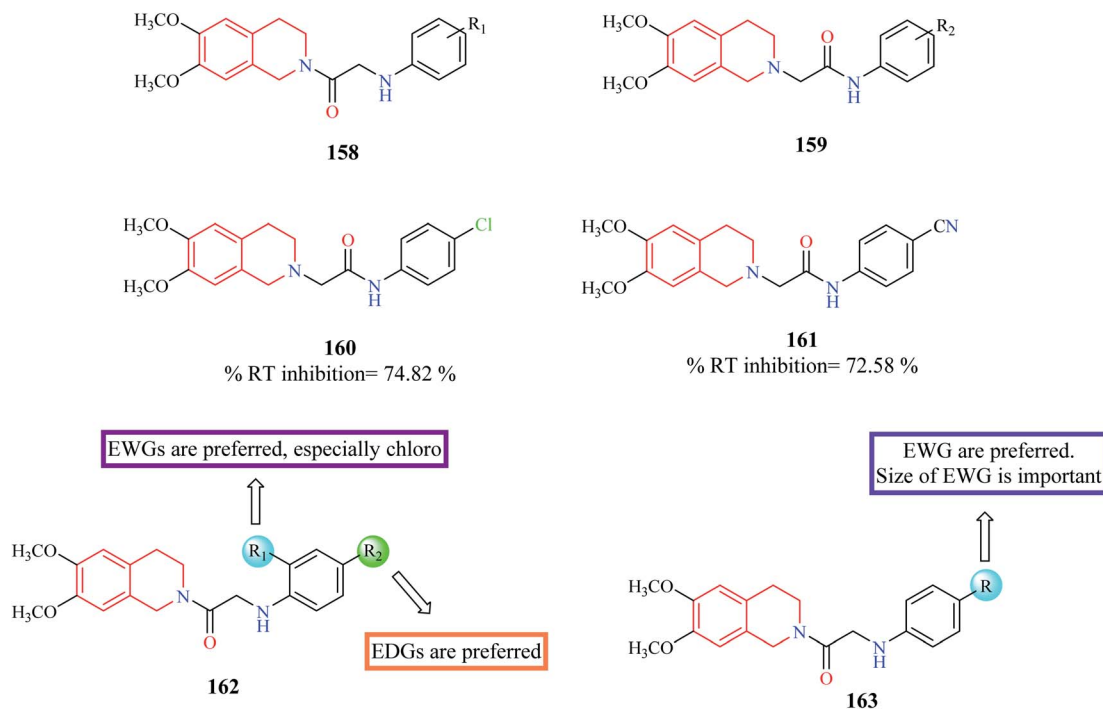


Fig. 12 SAR profile of *N*-substituted THIQ analogs as RT inhibitors.

(Fig. 18) exhibited good antileishmanial activity ( $IC_{50} = 7.62 \mu\text{M}$ ) against the amastigotes form of *Leishmania donovani* with a good selectivity index.

A series of novel THIQ analogs were synthesized and screened against the promastigote and amastigote forms of *L. infantum*.<sup>57</sup> The THIQ analogs exhibited weak to potent activity against both forms of the leishmanial parasite. Compounds **185** and **186** exhibited potent activity against the amastigotes with  $IC_{50}$  values of  $6.84 \mu\text{M}$  and  $11.35 \mu\text{M}$ , respectively.

### 3.6 Anti-trypanosomal activity

Cullen *et al.* synthesized novel THIQ analogs by derivatizing the core scaffold **187** (Fig. 19).<sup>58</sup> The synthesized analogs were screened for their inhibitory action against *Trypanosoma brucei rhodesiense*. Compounds **188–190** were found to exhibit potent activity antitrypanosomal activity. Preliminary SAR analysis revealed that compounds containing biphenyl methyl substitution at the phenolic OH displayed more potency and substitution at 1-position of THIQ nucleus had no effect on the antitrypanosomal activity.

### 3.7 Anti-schistosomal activity

Sadhu *et al.* synthesized novel praziquantel (PZQ) analogs with diversification at the aromatic and piperazine nucleus.<sup>59</sup> Most of the synthesized compounds lacked activity, however, compounds **191** and **192** (Fig. 20) were found to exhibit potent activity against *Schistosoma mansoni* with 90% lethal concentration ( $LC_{90}$ ) values of 10 and  $25 \mu\text{M}$ , respectively.

Duan and co-workers designed novel PZQ analogs by hybridizing PZQ with another established antischistosomal

drug, artemether.<sup>60</sup> Initially a simple derivative of PZQ, **193** was synthesized, after which the hybrid compounds **194** and **195** were synthesized. All three compounds were evaluated for their antischistosomal activity against both the juvenile and adult forms of *S. japonicum*. Compounds **193–195** exhibited potent activity against the adult form of the parasite, much better than the standard drug PZQ. They were also found to be equally effective against the juvenile form, reducing the worm vitality to 100% in 72 hours at  $15 \mu\text{M}$ . PZQ on the other hand wasn't effective at all. Compounds **193–195** were also evaluated for their worm reduction activity *in vivo*. All three compounds were moderately effective in reducing the worm load in mice. Importantly, compound **195** effectively reduced the worm load of both the adult and juvenile form of the parasite in mice, with a total worm reduction rate of 56.2% and 70.3%, respectively. Further *in vivo* studies demonstrated that compound **195** reduced the worm load by 60–85% in different developmental stages of the worm. Further dive into its mechanism of action revealed that compound **195** exhibited its activity by damaging the inner and outer walls of the worm tegument.<sup>61</sup> Further in-depth studies were also conducted to prove its prowess as an antischistosomal agent.<sup>62</sup> These compelling studies made compound **195** a possible drug candidate that can be explored further for the treatment of schistosomiasis.

A series of novel PZQ derivatives were designed and synthesized by substituting different groups on the aromatic ring of PZQ.<sup>63</sup> The synthesized compounds were evaluated against adult and juvenile forms of *S. japonicum in vitro*. A couple of compounds **196** and **197** (Fig. 21) exhibited potent anti-schistosomal activity. Compound **197** in particular, was equipotent as the standard drug PZQ. Compounds **196** and **197** were



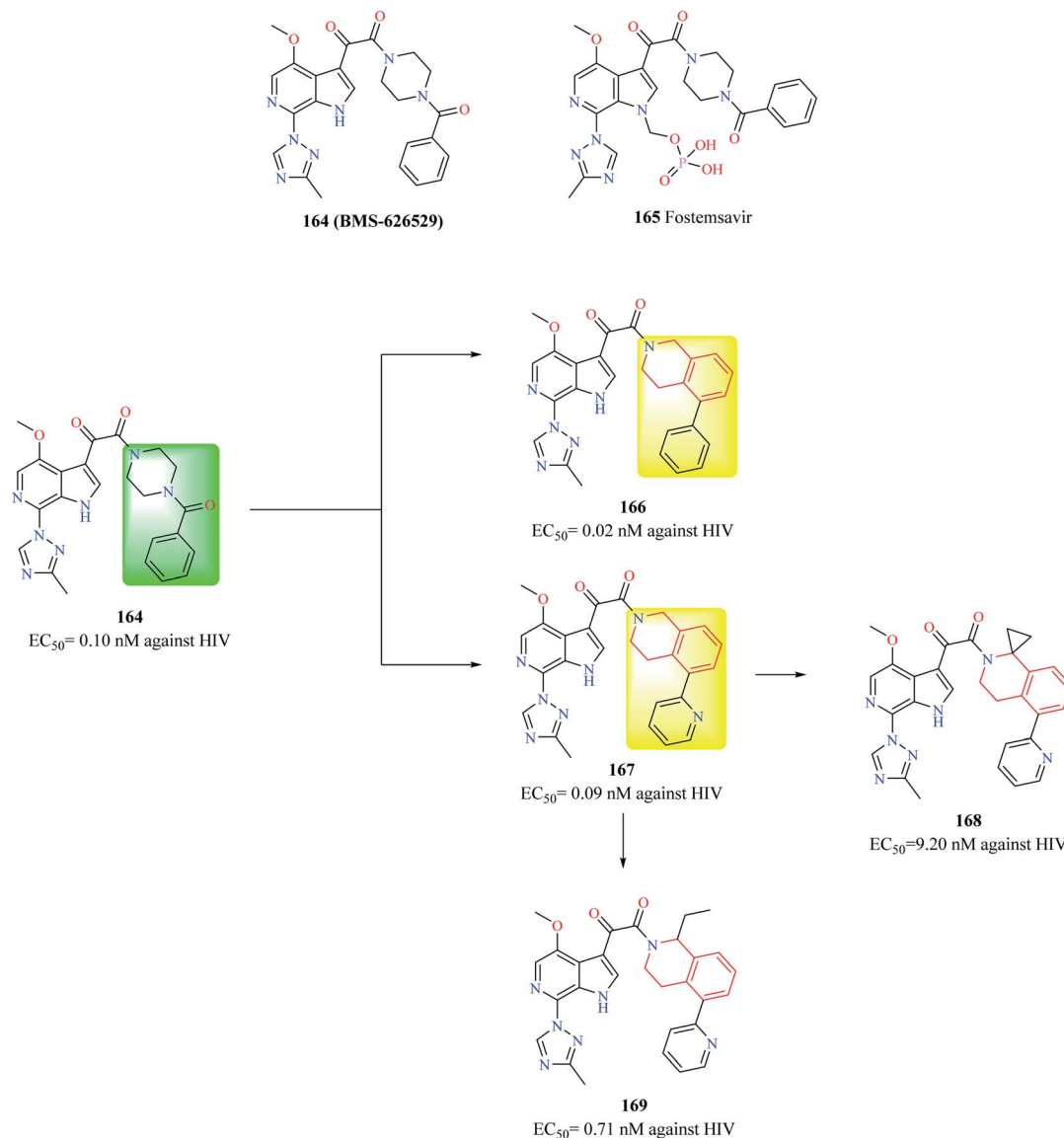


Fig. 13 Design of THIQ analogs as anti-HIV agents.

also effective against the juvenile form and compound **197** reduced the worm vitality to less than 10% at a concentration of 25  $\mu$ M at the end of 72 hours. Compounds **196** and **197** were also tested for their efficacy in mice harboring 42 day old *S. japonicum*. Compounds **196** and **197** reduced the worm count by 44.3% and 54.3% respectively.

Wang *et al.* designed and synthesized novel PZQ derivatives and explored their antischistosomal activity.<sup>64</sup> The compounds were designed by replacing the cyclohexane ring with different groups like an aliphatic chain, aromatic ring systems, aliphatic cyclic rings. The effect of the amide groups at positions 2 and 4 was also determined. Compound **199** (Fig. 22) containing

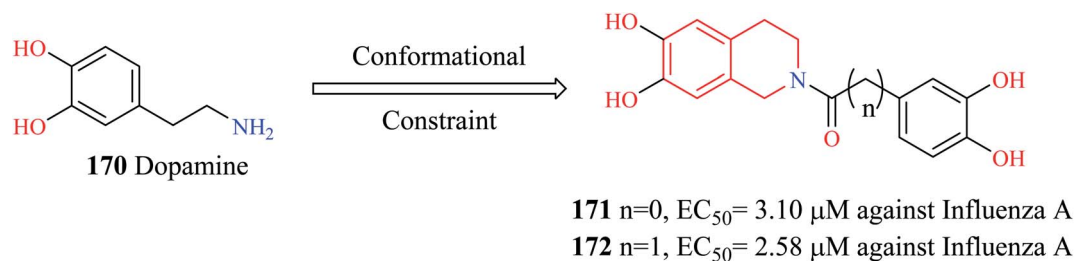


Fig. 14 Design of THIQ analogs as anti-influenza A agents.



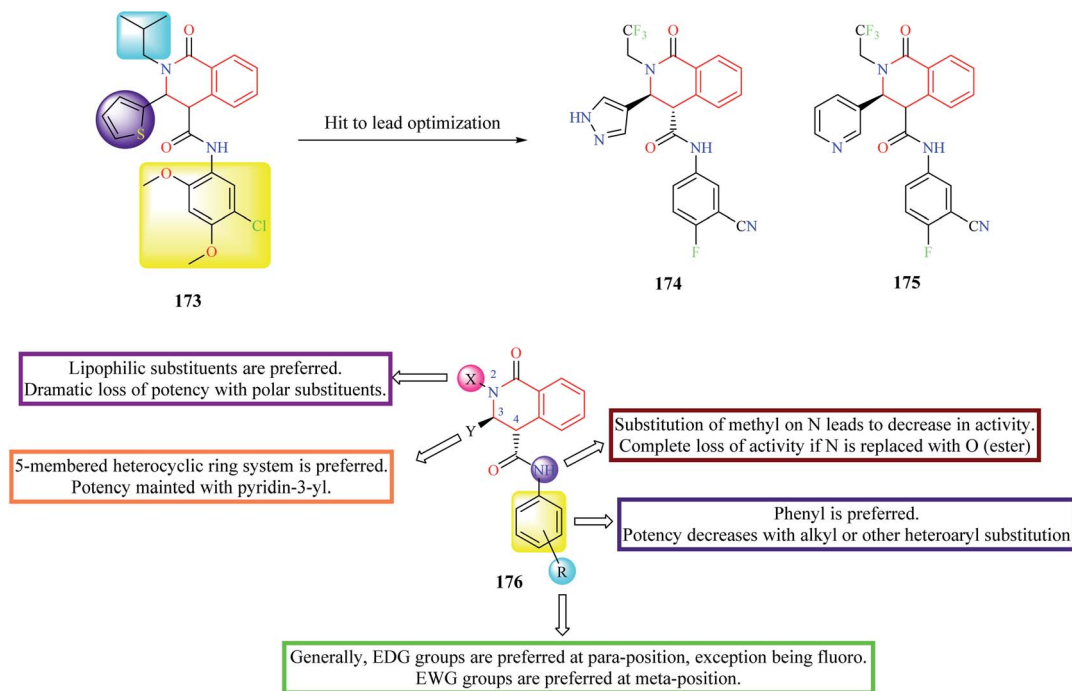


Fig. 15 Hit to lead optimization of compound **173** along with SAR profile.

a chloromethyl substituent was found to more potency than PZQ. Compound **199** was able to completely kill the worms at a concentration of 5  $\mu\text{M}$ . The SAR is discussed in Fig. 22.

Guglielmo and others employed molecular hybridization technique to design novel PZQ-furoxans as potential antischistosomal agents.<sup>65</sup> Furoxans are 1,2,5-oxadiazole-2-oxides that have been previously shown to be effective against schistosomiasis due to their NO donating capacity. Furoxan derivatives inhibit thioredoxin glutathione reductase (TGR), a multifunctional protein in the worms.<sup>66–69</sup> Therefore, at least theoretically, hybridizing the furoxan scaffold with PZQ may

lead to the development of potent antischistosomal agents. In the first series of hybrid compounds **201** (Fig. 23), the cyclohexyl group of PZQ was replaced with furoxans. In the second hybrid series **202**, the furoxan moiety was bridged to the 10<sup>th</sup> position of PZQ using appropriate linkers. The synthesized compounds were evaluated for their ability to inhibit *S. mansoni* (TGR) and for their worm-killing ability. Compounds **203** and **204** were found to exhibit potent activity against TGR ( $\text{IC}_{50} = 0.01 \mu\text{M}$  and 0.316  $\mu\text{M}$ , respectively). Both compounds **203** and **204** were also endowed with good worm-killing potency, in which compound **203** induced 80% of worm death in 144 h while compound **204**

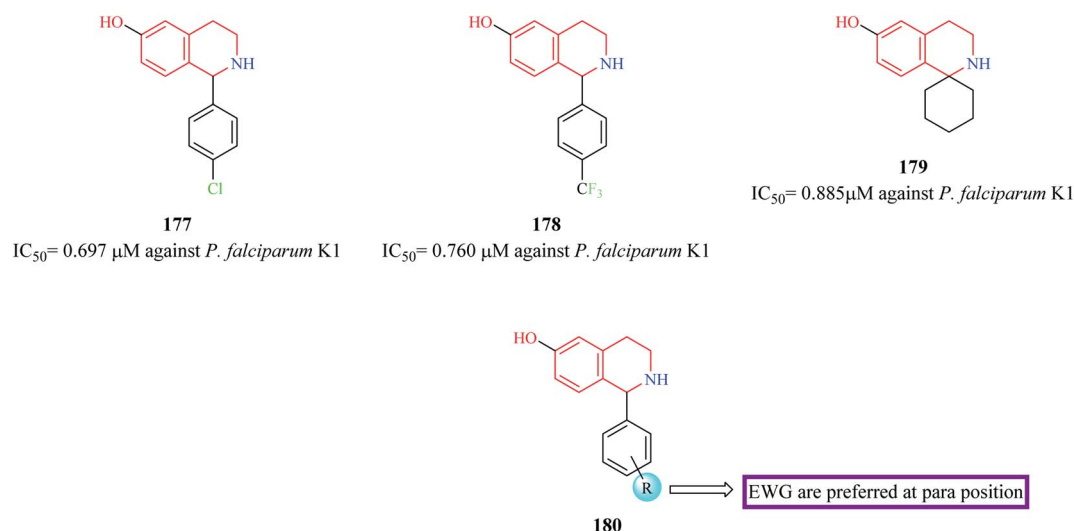
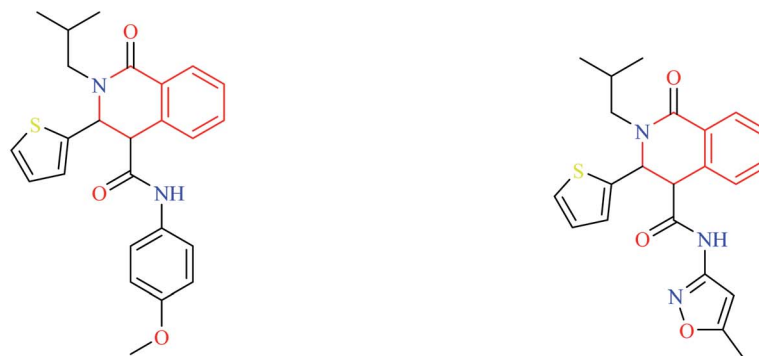


Fig. 16 Structure of THIQ analogs **177–179** as anti-malarial agents.

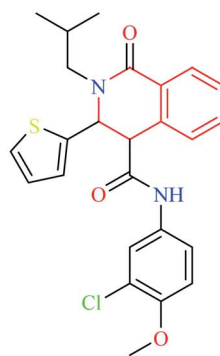


**181**

IC<sub>50</sub> = 0.133 μM against *P. falciparum* W2  
 = 0.120 μM against *P. falciparum* 3D7  
 = 3.57 μM against *P. falciparum* gametocytes

**182**

IC<sub>50</sub> = 0.132 μM against *P. falciparum* W2  
 = 0.123 μM against *P. falciparum* 3D7  
 = 4.42 μM against *P. falciparum* gametocytes

**183**

IC<sub>50</sub> = 0.070 μM against *P. falciparum* W2  
 = 0.117 μM against *P. falciparum* 3D7  
 = 3.43 μM against *P. falciparum* gametocytes

Fig. 17 Structure of anti-malarial compounds 181–183.

induced 100% worm death in 72 h. In comparison, PZQ exhibited only 40% worm death at the end of 144 h.

### 3.8 Anti-depressant activity

The antidepressant potential of 1-methyl THIQ 205 (Fig. 24) in animal models of depression was demonstrated by Antkiewicz-Michaluk and co-workers.<sup>70</sup> 1-Methyl THIQ administered at a dose of 10, 25, 50 mg kg<sup>-1</sup> i.p. caused a significant reduction of the immobility time in the forced swimming test (FST). 1-Methyl THIQ at a dose of 50 mg kg<sup>-1</sup> i.p. produced better activity than the standard drug imipramine (dose = 30 mg kg<sup>-1</sup> i.p.). The 1-methyl THIQ also significantly increased the swimming time (dose = 25, 50 mg kg<sup>-1</sup> i.p.) and climbing activity (dose = 50 mg kg<sup>-1</sup> i.p.) of the rats. 1-Methyl THIQ at the highest dose reduced the locomotor activity of rats like imipramine, thus ruling any psychostimulating activity. The neurochemical analysis revealed that 1-methyl THIQ produced

a significant elevation in the serotonin levels with a simultaneous reduction in its metabolite 5-hydroxy indole acetic acid (5-HIAA). Moreover, it also affected the dopamine metabolism; causing a decrease in the levels of 3,4-dihydroxyphenylacetic acid (DOPAC) with a significant increase in the levels of 3-methoxytyramine (3-MT). These effects of 1-methyl THIQ are attributed to the fact that it is a well-characterized inhibitor of monoamine oxidase (MAO).<sup>71</sup> Inhibition of MAO by 1-methyl THIQ causes elevation of serotonin in the rat striatum.<sup>72</sup> 1-Methyl THIQ has also been shown to inhibit the MAO-dependent oxidation of dopamine and shift its catabolism towards Catechol *O*-methyltransferase (COMT) dependent pathway. Such a shift in dopamine metabolism also reduces oxidative stress in the brain (due to MAO-dependent dopamine oxidation), which is also ascribed to be involved in the pathophysiology of depression.<sup>73,74</sup> Moreover, 1-methyl THIQ has also been demonstrated to be a scavenger of free radicals.<sup>75</sup> A Similar



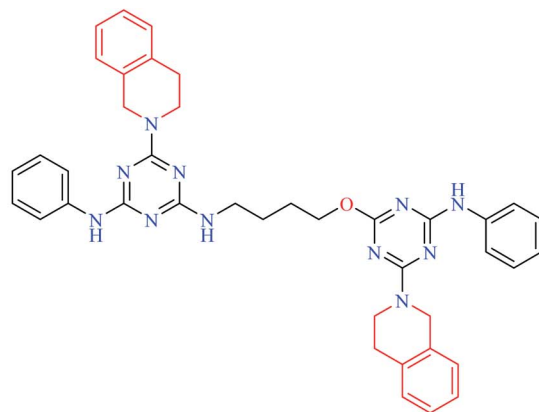
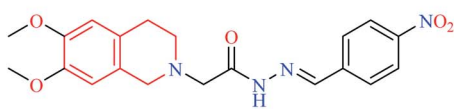
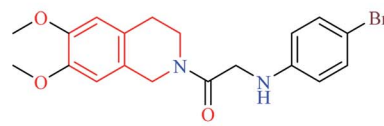
**184** $IC_{50} = 7.52 \mu\text{M}$  against *L. donovani* amastigotes**185** $IC_{50} = 6.84 \mu\text{M}$  against *L. infantum* amastigotes  
 $= 31.41 \mu\text{M}$  against *L. infantum* promastigotes**186** $IC_{50} = 11.35 \mu\text{M}$  against *L. infantum* amastigotes  
 $= 13.19 \mu\text{M}$  against *L. infantum* promastigotes

Fig. 18 Structure of anti-leishmanial THIQ analogs 184–186.

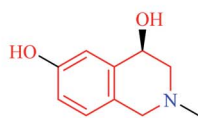
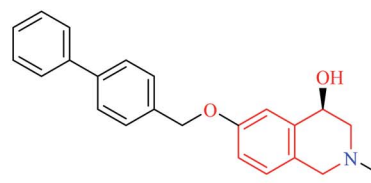
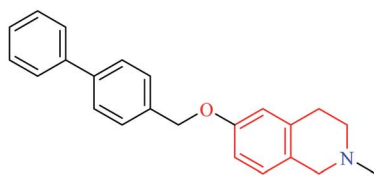
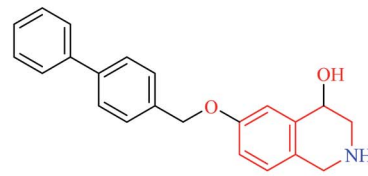
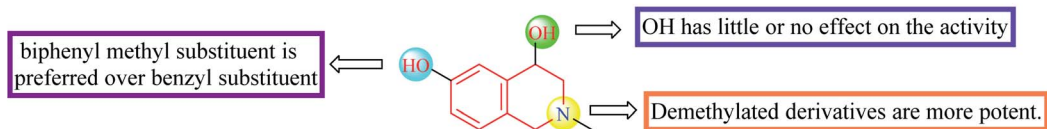
**187****188** $IC_{50} = 2.9 \mu\text{M}$  against *Trypanosoma brucei rhodesiense***189** $IC_{50} = 2.3 \mu\text{M}$  against *Trypanosoma brucei rhodesiense***190** $IC_{50} = 0.25 \mu\text{M}$  against *Trypanosoma brucei rhodesiense***187**

Fig. 19 SAR profile of 4,6-dihydroxy THIQ analogs.



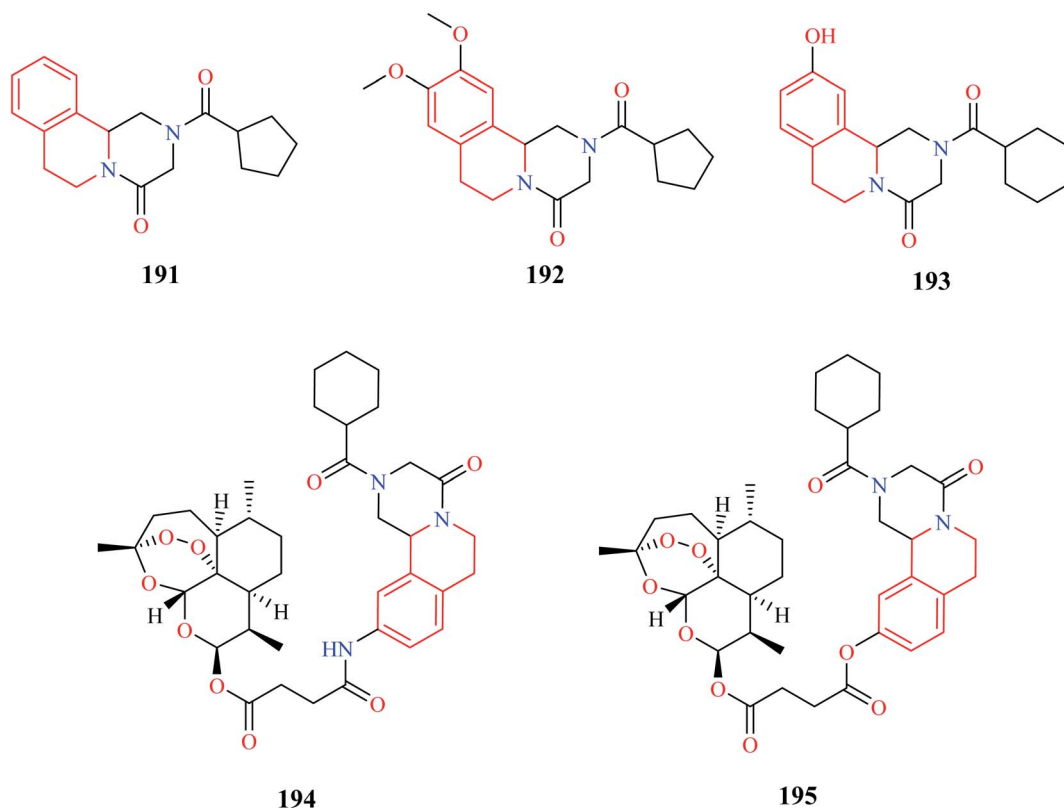


Fig. 20 Structure of anti-schistosomal PZQ derivatives.

antidepressant activity was also observed for the THIQ. THIQ administered at a dose of 25, 50 mg kg<sup>-1</sup> was found to significantly decrease the immobility time and increase the swimming activity of the rats in FST. Besides exhibiting its antidepressant activity in the FST model, administration of THIQ for about 3 weeks completely restored normal sucrose consumption in the rats that were subjected to the chronic mild stress (CMS) test.<sup>76</sup> Further studies also corroborated the antidepressant potential of THIQ and 1-methyl THIQ.<sup>77,78</sup> Additionally, 1-methyl THIQ was subjected to intense *in vitro*, *in vivo*, and *in silico* toxicity studies.<sup>79</sup> No significant toxicity was observed for 1-methyl

THIQ in the *in vitro* and *in vivo* toxicity studies. The unique mechanism of action(s) of 1-methyl THIQ in depression supplemented with a lack of significant toxicity makes it an interesting antidepressant drug candidate for further studies.

Nomifensine **206** is a norepinephrine and dopamine reuptake inhibitor that was used as an antidepressant in the 1970s. However, it was withdrawn from the market in the 1980s due to its toxicity. The aniline moiety in the nomifensine was attributed to the generation of toxic metabolites.<sup>80-82</sup> Molino and co-workers designed a series of THIQ analogs based on the structure of nomifensine as dual norepinephrine and dopamine

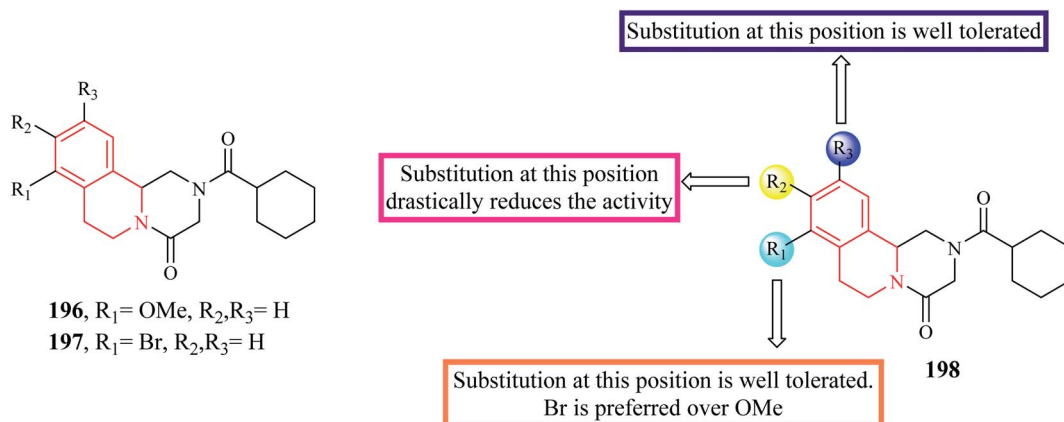


Fig. 21 SAR profile of PZQ derivatives (substitutions on phenyl group).



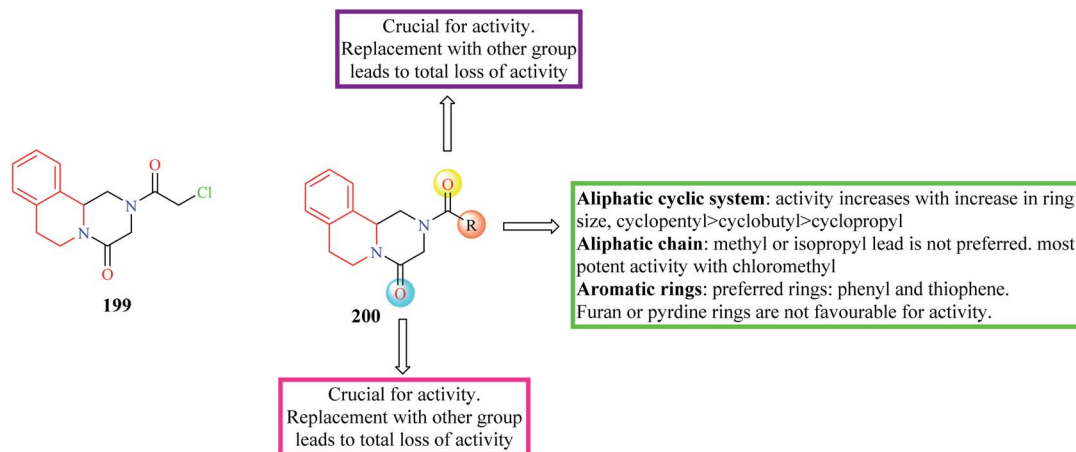


Fig. 22 SAR profile of PZQ derivatives (replacement of cyclohexane group).

reuptake inhibitors.<sup>83</sup> Removal of the amino group and optimization of the compounds around the THIQ core and 4-phenyl moiety resulted in the generation of compounds **207–209** (Fig. 25) with good potency against norepinephrine transporter (NET) and dopamine transporter (DAT). Compound **209** displayed significant NET occupancy (49%) in the *ex vivo* binding assay. Compound **209** was subjected to further studies wherein it was found to be selective for NET and DAT without any off-

target activity. However, compound **209** was found to inhibit the CYP2D6 with moderate potency ( $IC_{50} = 0.48 \mu M$ ), which might result in unwanted drug–drug interactions.

In subsequent studies, novel THIQ analogs were designed by taking cues from compound **209**.<sup>84</sup> This series of compounds explored the substitution of different heterobicyclic groups on the 4-position of the THIQ nucleus. Substitution with heterobicyclic groups gave rise to compounds that were capable of

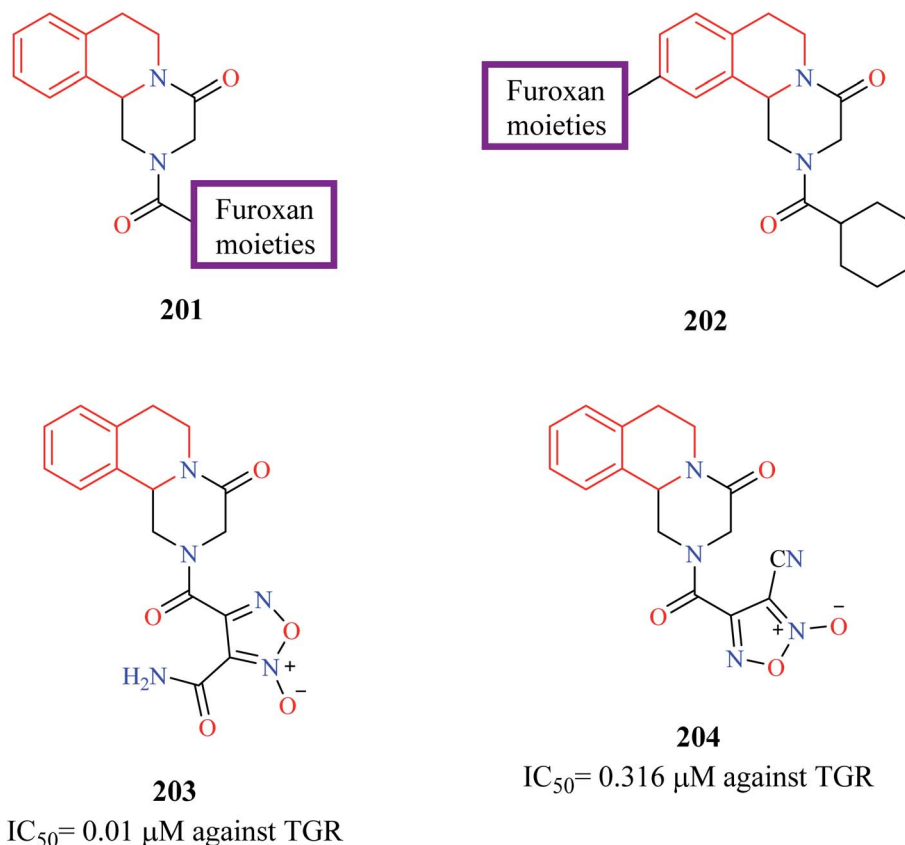


Fig. 23 Structure of anti-schistosomal PZQ-furoxan hybrid analogs.



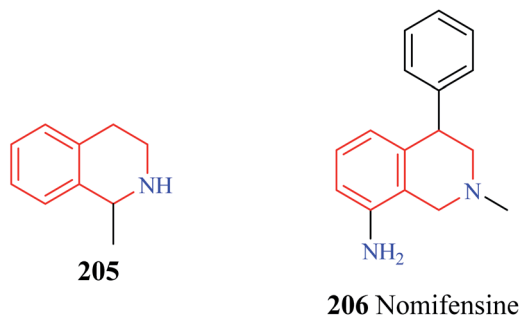


Fig. 24 Structure of 1-methyl THIQ 205 and nomifensine 206.

inhibiting NET, DAT, and Serotonin transporter (SERT), thus giving rise to triple reuptake inhibitors. In general, the (+) enantiomers were found to be more potent than their counterpart. In general, THIQs substituted with indole, benzofuran, and benzothiophene were found to be superior triple reuptake inhibitors with compound 211 (Fig. 26) being the most potent of them all. It was also found to exhibit significant potency against CYP2D6 ( $IC_{50} = 0.8 \mu\text{M}$ ). Different analogs of compound 211 were then synthesized by substituting different groups on the 7-

position of the THIQ core. Optimization of compound 211 led to the development of compound 212 with potent activity against all three transporters with low activity against CYP2D6 ( $IC_{50} = 11 \mu\text{M}$ ). Compound 212 (dose =  $3 \text{ mg kg}^{-1} \text{ p/o}$ ) was also found to have good occupancy at SERT (95%), DAT (77%), NET (98%) in *ex vivo* binding assays. Compound 212 was found to possess significant antidepressant activity in FST and Tail suspension models, reducing the immobility time in both models. However, metabolic profiling of compound 212 led to the discovery of a significant metabolite compound 213 that was found to possess equal potency against the three transporters as that of compound 212. Further studies corroborated that compound 213 might contribute to the *in vivo* pharmacology of compound 212. However, compound 213 was found to have an affinity for CYP2D6 ( $IC_{50} = 1 \mu\text{M}$ ), therefore susceptible to drug-drug interactions. The SAR of these groups of compounds has been summarized in Fig. 26.

### 3.9 Anti-Alzheimer activity

Sukumarapillai and others designed a series of THIQ analogs and evaluated their inhibitory potential against cholinesterases: acetylcholinesterase (AChE) and butyrylcholinesterase (BChE),

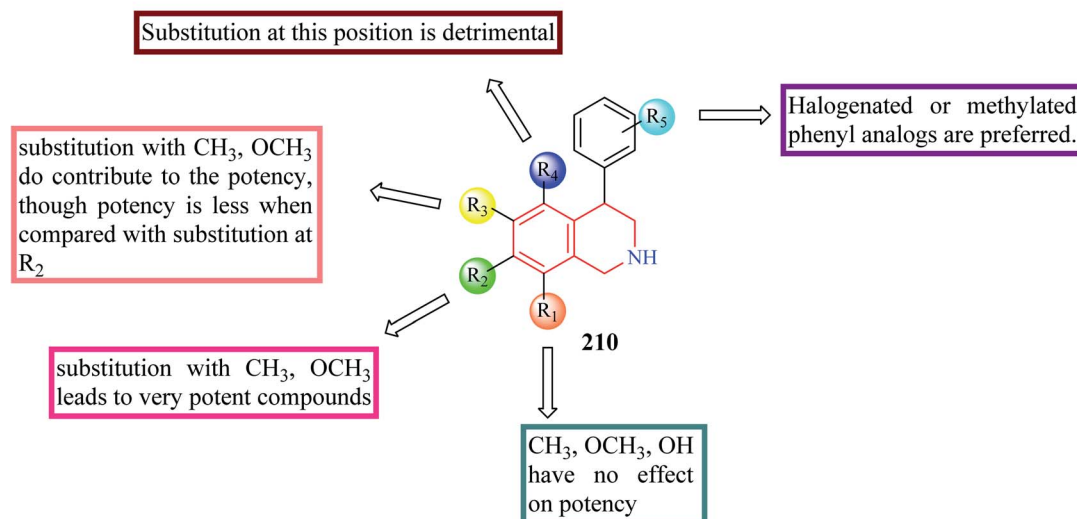
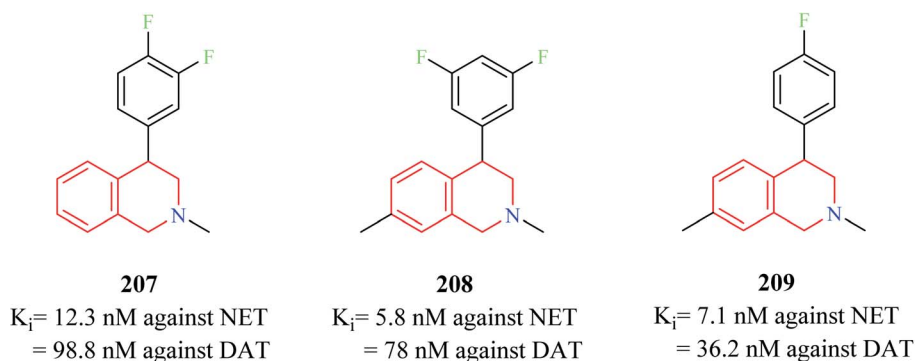


Fig. 25 SAR profile of dual reuptake inhibitory THIQ derivatives.



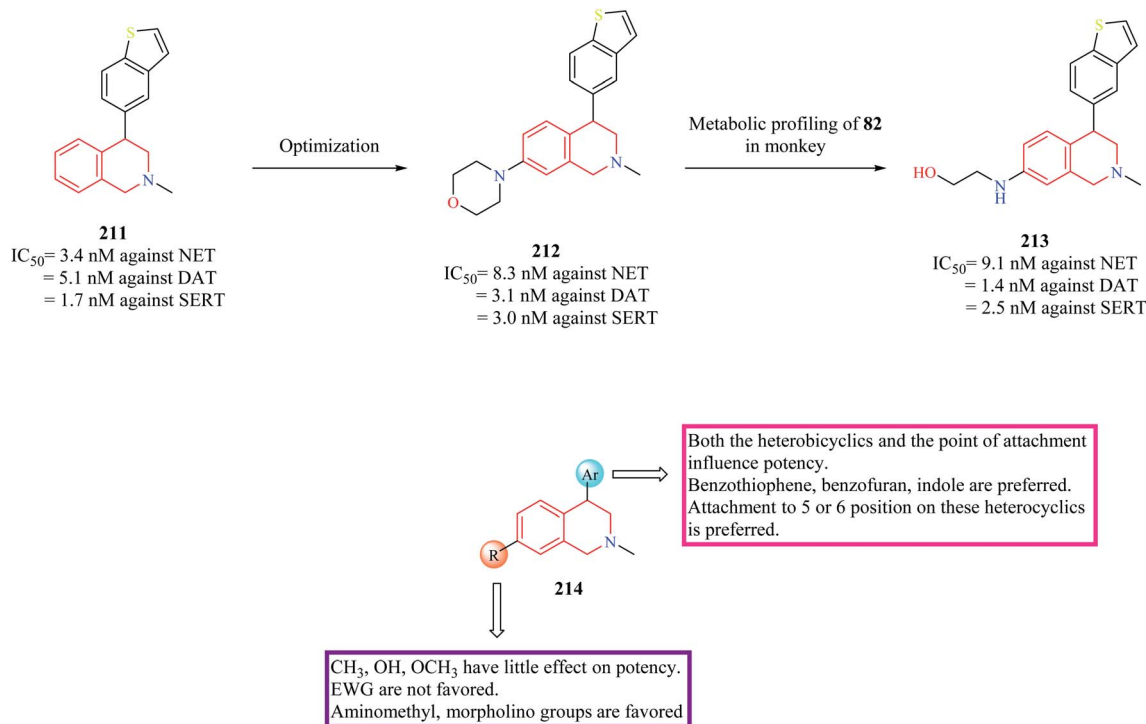


Fig. 26 SAR profile of triple reuptake inhibitors.

a widely explored target for the development of anti-Alzheimer agents.<sup>85</sup> A couple of compounds **215** and **216** (Fig. 27) were found to exhibit good inhibitory potential against both the enzymes with their activity being more pronounced against BChE. Enzyme kinetic studies revealed that the compounds exhibited a mixed-mode of inhibition against both the enzymes. Molecular docking studies were performed to determine the probable binding mode of the compounds. Compound **215** was

found to exhibit hydrophobic and hydrogen bond interactions with the active site residues of the enzymes. Sudhapriya *et al.* synthesized triazolo-benzodiazepino-THIQ fused analogs as potential AChE inhibitors. Compound **217** was found to potently inhibit AChE with an  $IC_{50}$  value of 0.25  $\mu$ M.<sup>86</sup>

Since Alzheimer's disease (AD) is a multifactorial disease involving intricate targets and molecular pathways, the development of ligands that can engage more than one target seems

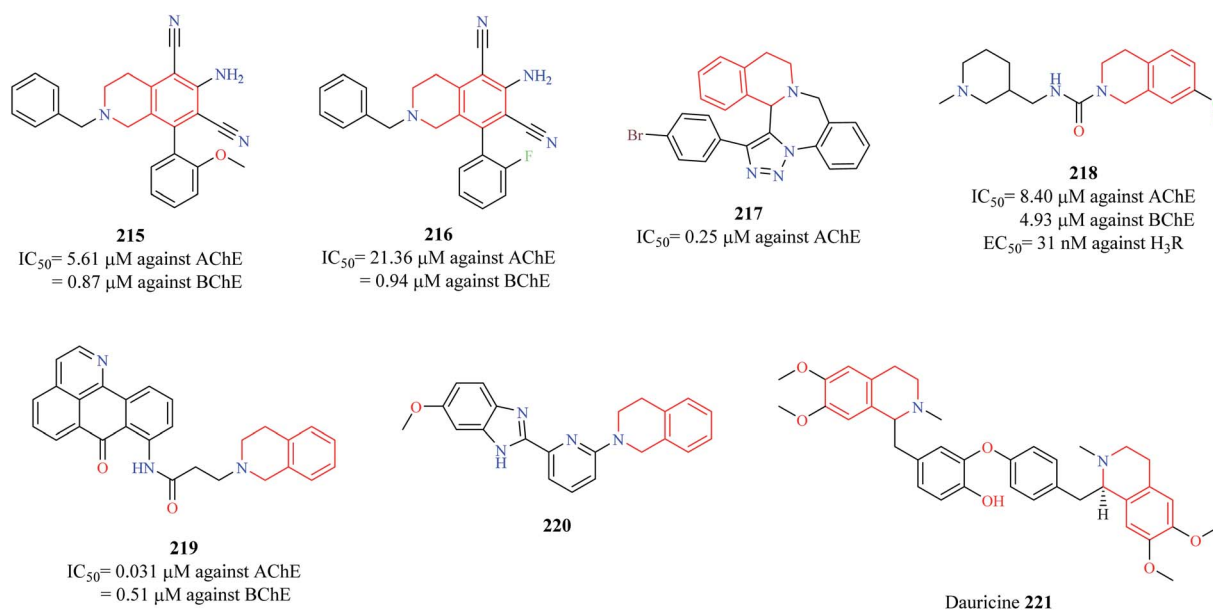


Fig. 27 Structure of anti-Alzheimer THIQ analogs **215**–**221**.



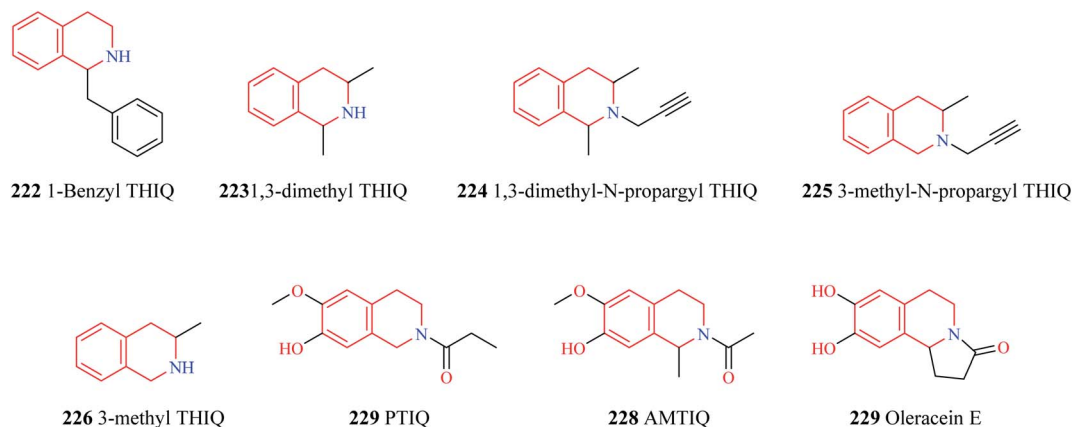


Fig. 28 Structure of THIQ analogs 222–229.

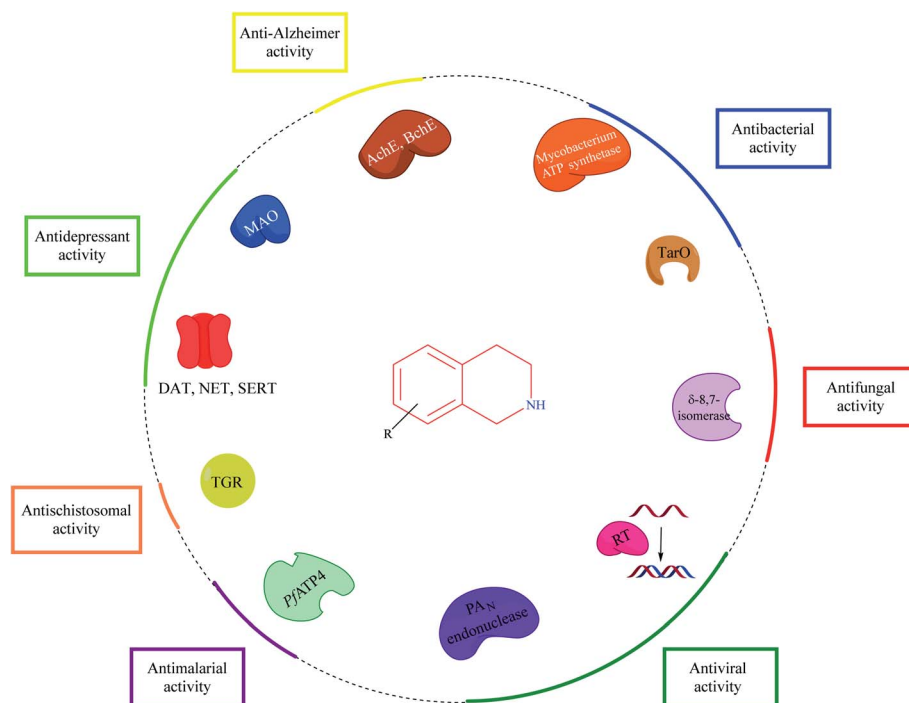


Fig. 29 Potential targets and their associated activities for THIQ based analogs.

an interesting approach to combat AD. A similar strategy was taken up by Ghamari and co-workers<sup>87,88</sup> wherein they tested the potential of compound **218** to act as cholinesterase inhibitor and Histamine 3 receptor (H3R) antagonist, an emerging target for the management of AD.<sup>89,90</sup> Compound **218** was found to exhibit nanomolar potency against the H3R ( $EC_{50} = 31$  nM) and micromolar potencies against AChE ( $IC_{50} = 8.40$   $\mu$ M) and BChE ( $IC_{50} = 4.93$   $\mu$ M) with no significant impact on the viability of CHO-K1 cells. Molecular docking studies revealed that compound **218** had a similar binding pattern as that of donepezil in the active site of AChE with THIQ ring exhibiting a  $\pi$ - $\pi$  stacking and hydrophobic interaction with Trp286 and Try341 respectively. Additionally, the nitrogen of the THIQ ring system was found to have a hydrogen bond interaction with Tyr124.

Chen and co-workers designed a new series of oxoisoaporphine-tetrahydroisoquinoline analogs based on the concept of molecular hybridization as multi-target directed ligands (MTDLs) in AD.<sup>91</sup> Compound **219** exhibited the following properties: (i) strongly suppressed the production of NO-induced by LPS in BV-2 microglia and RAW 264.7 macrophage (ii) compound **219** also suppressed the expression of iNOS in RAW 264.7 macrophage cells (iii) compound **219** was also shown to suppress the LPS-induced production of pro-inflammatory cytokines such as TNF- $\alpha$  and IL- $\beta$  (iv) compound **219** was able to reduce A $\beta_{42}$  levels by 37.6% (v) exhibited potent inhibitory activity against AChE ( $IC_{50} = 0.031$   $\mu$ M) and BChE ( $IC_{50} = 0.51$   $\mu$ M) (vi) caused a significant delay in paralysis (due to A $\beta_{1-42}$  toxicity) in *C. elegans* GMC101 *in vivo*



model. These results suggest that compound **219** may be a promising anti-Alzheimer agent that needs further exploration. A similar strategy was conceptualized by Fang *et al.* wherein they developed THIQ-benzimidazole hybrids as MTDLs as a potential treatment strategy for AD.<sup>92</sup> Among them, compound **220** was found to possess good anti-neuroinflammatory property ( $IC_{50} = 5.07 \mu\text{M}$  against NO production) by inhibiting the production of iNOS and pro-inflammatory cytokines (TNF- $\alpha$  and IL-1 $\beta$ ) in BV-2 cells. It was also shown to possess moderate inhibitory activity against  $\beta$ -amyloid precursor protein cleaving enzyme 1 (BACE1) and potent neuroprotective activity against glutamate-induced cell death in HT22 cells by inhibiting the production of reactive oxygen species (ROS) and increasing the levels of glutathione. It possessed good blood-brain barrier (BBB) penetration ability, making it an interesting candidate for further development.

Dauricine **221** is a benzyl THIQ alkaloid that has been conferred with neuroprotective effects in AD. Different mechanisms have been proposed for its neuroprotective effects. It was found to reduce A $\beta$  accumulation by activating the X-box binding protein 1 (XBP-1) and eukaryotic translation initiation factor (eIF2 $\alpha$ ) arms of the unfolded protein responses (UPR), which results in the clearance of A $\beta$  oligomers and their associated toxicities.<sup>93</sup> The anti-apoptotic and strong antioxidant properties of dauricine also accounted for its neuroprotective effects in AD.<sup>94</sup> Further studies indicated that it reduced tau phosphorylation along with A $\beta$  plaque formation by altering UPR, mitochondrial function, and ROS clearance.<sup>95</sup>

### 3.10 Anti-Parkinson activity

The endogenous THIQs – 1-benzyl THIQ **222** (Fig. 28) and 1-methyl THIQ **205** have contrasting effects in Parkinson's disease (PD). 1-Benzyl THIQ **222** potentiates the metabolism of dopamine, increases the production of free radicals by activating the dopamine oxidation pathway and inhibiting dopamine metabolism *via* the COMT pathway, and induces cell death *via* apoptotic mechanisms.<sup>96–98</sup> It is also regarded as an etiological factor in idiopathic PD. The levels of 1-benzyl THIQ in cerebrospinal fluid (CSF) were found to be significantly higher (about three times) in PD patients than in control patients.<sup>99</sup> Studies have demonstrated that chronic administration of 1-benzyl THIQ produces parkinsonian-like symptoms in primates and rodents highlighting its neurotoxic effects.<sup>99–101</sup> In contrast, 1-methyl THIQ, another endogenous THIQ, has been demonstrated to translate its neuroprotective role in animal models of PD as well. Studies have demonstrated that acute and chronic administration of 1-methyl THIQ completely antagonizes the neurotoxic effect of 1-benzyl THIQ on dopaminergic neurons. A similar neuroprotective activity was also observed for THIQ.<sup>102,103</sup> Furthermore, chronic administration of both THIQ and 1-methyl THIQ have been shown to offer protection against 6-hydroxy dopamine-induced disturbances in the dopaminergic neurons.<sup>104,105</sup> Several other synthetic THIQs have also been shown to exert neuroprotective effects in animal models of PD. Taguchi and co-workers evaluated the neuroprotective effects of 1,3-dimethyl THIQ **223** and 1,3-dimethyl-*N*-propargyl THIQ **224**

on 1-methyl-4-phenyl-1,2,3,6-tetrahydropyridine (MPTP) and methyl-4-phenylpyridinium ion (MPP<sup>+</sup>), an active metabolite of MPTP, induced PD like symptoms in mice.<sup>106</sup> Though 1,3-dimethyl THIQ did not offer much neuroprotective effects, 1,3-dimethyl-*N*-propargyl THIQ was found to prevent the adverse events induced by MPTP and MPP<sup>+</sup>. Stereoselectivity had an important role to play as *cis* and *trans* isomers of 1,3-dimethyl-*N*-propargyl THIQ was found to have different neuroprotective functions. Both the isomers were found to prevent MPTP-induced bradykinesia, tyrosine hydroxylase (TH) positive cell loss, and decreased dopamine levels with the *trans* isomer of 1,3-dimethyl-*N*-propargyl THIQ exhibiting superior activity than its counterpart. However, the *cis* isomer was found to afford superior protection against MPP<sup>+</sup> induced cell death than the *trans* isomer. In a similar study, 3-methyl-*N*-propargyl-THIQ **225** prevented MPTP induced adverse events in mice while a THIQ analog without the propargyl group, 3-methyl THIQ **226** was found to have only weak activity against MPTP induced PD like symptoms.<sup>107</sup> These studies shed light on the importance of the propargyl group in the neuroprotective activity. It is speculated that compounds like **224** and **225** exhibit its anti-parkinsonism action by inhibiting the neurotoxicity caused by MPP<sup>+</sup> by competing with MPP<sup>+</sup> in the catecholamine uptake sites.<sup>107</sup> However, further studies are required to elucidate the exact role of the propargyl group in neuroprotection. Son and others disclosed the promising potential of PTIQ **227** in PD.<sup>108</sup> Compound **227** suppressed the production of matrix metalloproteinase-3 (MMP-3, which plays an important role in dopaminergic neurodegeneration) in the CATH.a cell and also offered cytoprotection. Compound **227** also downregulated MMP-3, COX-2, and other proinflammatory cytokines like IL-1 $\beta$ , TNF- $\alpha$  in BV-2 microglial cells activated with Lipopolysaccharides (LPS). Compound **227** also attenuated the adverse events induced by MPTP in mice. Moreover, compound **227** was also bestowed with the following pharmacokinetic properties – (i) compound **227** was stable against liver microsomal enzymes (ii) exhibited high  $IC_{50}$  values against CYP450 enzymes (iii) no side effect against hERG channel (iv) no cytotoxicity towards liver cells (v) no lethality to animals at 1000 mg kg<sup>-1</sup> i.p. (vi) readily penetrates BBB. Similar pharmacological effects were observed for AMTIQ **228**, a derivative of PTIQ. Compound **228** suppressed inflammatory responses in activated microglial BV-2 cells and attenuated the effects of MPTP (motor deficits and dopamine neurodegeneration) in mice. Compound **228** was stable against liver microsomes, lacked CYP450 inhibitory effect, and was also demonstrated to possess better BBB penetration than PTIQ.<sup>109</sup> Oleracein E **229** a naturally occurring THIQ analog was demonstrated to provide neuroprotection against rotenone-induced PD in cell and animal models.<sup>110</sup> Oleracein E was found to improve the motor functions in a PD mouse model, preserved and maintained TH positive neurons, and density of dopaminergic fibers in the substantia nigra pars compacta. Further mechanistic studies revealed that oleracein E exhibits its neuroprotective effects in cell and animal models *via* diverse mechanisms like scavenging free radicals and reducing oxidative stress, downregulating the phosphorylation of extracellular regulated kinases (ERKs), and inhibiting neuronal apoptosis.



## 4. Conclusion

THIQ is a privileged scaffold present in a number of clinically used drug molecules. The information amassed in this review article sheds light on the biological potential and SAR of THIQ based analogs across different facets of diseases. Various strategies for the construction of the THIQ core scaffold with special emphasis on multi-component reactions (MCR) are discussed.

Though Pictet–Spengler condensation and Bischler–Nepieralski reaction are the most commonly used synthesis strategies for constructing the THIQ core, MCR provides an opportunity to explore the chemical space to synthesize diverse THIQ analogs. Mechanistically, THIQ analogs exhibit their pharmacological properties by diverse mechanisms as described in Fig. 29.

Importantly, THIQs showed a profound effect on the central nervous system. Endogenous amines like 1-methyl THIQ and other synthetic THIQ analogs have been demonstrated to possess good neuroprotective properties, which have been shown to alleviate symptoms of depression and Parkinson's disease in animal models. However, there is still a lot to explore about these derivatives like delineating the importance of propargyl group in neuroprotection. Emerging drug discovery paradigm like MTDLs, consisting of THIQ based hybrid analogs, is a promising strategy for the development of novel anti-Alzheimer agents that needs further exploration. Drug design strategies like structure-based drug design, ligand-based drug design, fragment-based drug design, and molecular hybridization could be employed for the design of novel THIQ analogs against various ailments.

Future medicinal chemistry efforts could be targeted to improve the potency and pharmacokinetic properties of existing THIQ analogs and unearth the mechanistic basis of activity at the molecular level. Medicinal chemistry strategies like bio-isosteric replacement, scaffold hopping, SAR among others could be employed for the optimization of identified lead compounds in order to enter the clinical trial phases of drug discovery. The synthetic ease combined with the nucleophilicity of the secondary nitrogen makes it possible for hybridizing the THIQ core with other privileged heterocyclic scaffolds for developing potent and effective hybrid analogs.

## Conflicts of interest

The authors have no conflicts of interest to declare.

## Acknowledgements

SM and KVGK thank the Department of Biotechnology for the research grant. This work was carried under the grant of the Department of Biotechnology, Indo-Spain, New Delhi. (Ref. No. BT/IN/Spain/39/SM/2017-2018). BKK is thankful to the Ministry of Tribal Affairs, Government of India for providing financial assistance (Award no. 201920-NFST-TEL-01497). SM and BKK thank BITS-Pilani, Pilani campus for providing adequate facilities like access to scientific journals to do this review study.

## References

- J. D. Scott and R. M. Williams, *Chem. Rev.*, 2002, **102**, 1669–1730.
- R. K. Tiwari, D. Singh, J. Singh, A. K. Chhillar, R. Chandra and A. K. Verma, *Eur. J. Med. Chem.*, 2006, **41**, 40–49.
- J. Zhu, J. Lu, Y. Zhou, Y. Li, J. Cheng and C. Zheng, *Bioorg. Med. Chem. Lett.*, 2006, **16**, 5285–5289.
- A. Kumar, S. B. Katiyar, S. Gupta and P. M. S. Chauhan, *Eur. J. Med. Chem.*, 2006, **41**, 106–113.
- X. H. Liu, J. Zhu, A. na Zhou, B. A. Song, H. L. Zhu, L. S. Bai, P. S. Bhadury and C. X. Pan, *Bioorg. Med. Chem.*, 2009, **17**, 1207–1213.
- J. J. Swidorski, Z. Liu, Z. Yin, T. Wang, D. J. Carini, S. Rahematpura, M. Zheng, K. Johnson, S. Zhang, P. F. Lin, D. D. Parker, W. Li, N. A. Meanwell, L. G. Hamann and A. Regueiro-Ren, *Bioorg. Med. Chem. Lett.*, 2016, **26**, 160–167.
- M. E. Zarranz De Ysern and L. A. Ordoñez, *Prog. Neuro-Psychopharmacol.*, 1981, **5**, 343–355.
- I. P. Singh and P. Shah, *Expert Opin. Ther. Pat.*, 2017, **27**, 17–36.
- A. Pictet and T. Spengler, *Ber. Dtsch. Chem. Ges.*, 1911, **44**, 2030–2036.
- W. M. Whaley and T. R. Govindachari, in *Organic Reactions*, John Wiley & Sons, Inc., Hoboken, NJ, USA, 2011, pp. 151–190.
- C. Kuhakarn, N. Panyachariwat and S. Ruchirawat, *Tetrahedron Lett.*, 2007, **48**, 8182–8184.
- C. Gremmen, M. J. Wanner and G. J. Koomen, *Tetrahedron Lett.*, 2001, **42**, 8885–8888.
- E. Mons, M. J. Wanner, S. Ingemann, J. H. Van Maarseveen and H. Hiemstra, *J. Org. Chem.*, 2014, **79**, 7380–7390.
- E. Awuah and A. Capretta, *J. Org. Chem.*, 2010, **75**, 5627–5634.
- S. Nagubandi and G. Fodor, *J. Heterocycl. Chem.*, 1980, **17**, 1457–1463.
- M. Nicoletti, D. O'Hagan and A. M. Z. Slawin, *J. Chem. Soc., Perkin Trans. 1*, 2002, **2**, 116–121.
- M. Mihoubi, N. Micale, A. Scala, R. M. Jarraya, A. Bouaziz, T. Schirmeister, F. Risitano, A. Piperno and G. Grassi, *Molecules*, 2015, **20**, 14902–14914.
- M. Mottinelli, M. Sinreih, T. L. Rižner, M. P. Leese and B. V. L. Potter, *ChemMedChem*, 2020, 1–34.
- C. E. Puerto Galvis and V. V. Kouznetsov, *J. Org. Chem.*, 2019, **84**, 15294–15308.
- P. Pieper, E. McHugh, M. Amaral, A. G. Tempone and E. A. Anderson, *Tetrahedron*, 2020, **76**, 130814.
- L. Weber, *Curr. Med. Chem.*, 2002, **9**, 2085–2093.
- P. Slobbe, E. Ruijter and R. V. A. Orru, *MedChemComm*, 2012, **3**, 1189–1218.
- D. Insuasty, J. Castillo, D. Becerra, H. Rojas and R. Abonia, *Molecules*, 2020, **25**, 1–71.
- L. Rong, L. Gao, H. Han, H. Jiang, Y. Dai and S. Tu, *Synth. Commun.*, 2010, **40**, 289–294.
- K. Balamurugan, V. Jeyachandran, S. Perumal and J. C. Menéndez, *Tetrahedron*, 2011, **67**, 1432–1437.
- D. L. Priebbenow, F. M. Pfeffer and S. G. Stewart, *Eur. J. Org. Chem.*, 2011, 1632–1635.



- 27 J. Jiang, X. Ma, C. Ji, Z. Guo, T. Shi, S. Liu and W. Hu, *Chem.–Eur. J.*, 2014, **20**, 1505–1509.
- 28 A. H. Shinde, N. Archith, S. Malipatel and D. S. Sharada, *Tetrahedron Lett.*, 2014, **55**, 6821–6826.
- 29 L. Henderson, D. W. Knight and A. C. Williams, *Tetrahedron Lett.*, 2012, **53**, 4657–4660.
- 30 T. Ogata, T. Kimachi, K. I. Yamada, Y. Yamamoto and K. Tomioka, *Heterocycles*, 2012, **86**, 469–485.
- 31 S. Tussing, M. Ohland, G. Wicker, U. Flörke and J. Paradies, *Dalton Trans.*, 2017, **46**, 1539–1545.
- 32 A. V. Murashkina, A. Y. Mitrofanov, Y. K. Grishin, V. B. Rybakov and I. P. Beletskaya, *ChemistrySelect*, 2018, **3**, 6810–6813.
- 33 X.-J. Dai, O. D. Engl, T. León and S. L. Buchwald, *Angew. Chem.*, 2019, **131**, 3445–3449.
- 34 J. D. Guzman, T. Pesnot, D. A. Barrera, H. M. Davies, E. McMahon, D. Evangelopoulos, P. N. Mortazavi, T. Munshi, A. Maitra, E. D. Lamming, R. Angell, M. C. Gershater, J. M. Redmond, D. Needham, J. M. Ward, L. E. Cuca, H. C. Hailes and S. Bhakta, *J. Antimicrob. Chemother.*, 2014, **70**, 1691–1703.
- 35 M. A. Farha, K. Koteva, R. T. Gale, E. W. Sewell, G. D. Wright and E. D. Brown, *Bioorg. Med. Chem. Lett.*, 2014, **24**, 905–910.
- 36 S. Murugavel, N. Manikandan, D. Lakshmanan, K. Naveen and P. T. Perumal, *J. Chil. Chem. Soc.*, 2015, **60**, 3015–3020.
- 37 K. Bielawski, K. Leszczyńska, Z. Kałuża, A. Bielawska, O. Michalak, T. Daniluk, O. Staszewska-Krajewska, A. Czajkowska, N. Pawłowska and A. Gornowicz, *Drug Des., Dev. Ther.*, 2017, **11**, 2015–2028.
- 38 A. Zablotskaya, I. Segal, A. Geronikaki, I. Shestakova, V. Nikolajeva and G. Makarenkova, *Pharmacol. Rep.*, 2017, **69**, 575–581.
- 39 A. Zablotskaya, I. Segal, G. Kazachonokh, Y. Popelis, I. Shestakova and V. Nikolajeva, *Silicon*, 2018, **10**, 1129–1138.
- 40 G. L. Lu, A. S. T. Tong, D. Conole, H. S. Sutherland, P. J. Choi, S. G. Franzblau, A. M. Upton, M. U. Lotlikar, C. B. Cooper, W. A. Denny and B. D. Palmer, *Bioorg. Med. Chem.*, 2020, **28**, 115784.
- 41 J. Krauss, C. Müller, J. Kießling, S. Richter, V. Staudacher and F. Bracher, *Arch. Pharm.*, 2014, **347**, 283–290.
- 42 T. R. Sutariya, B. M. Labana, N. J. Parmar, R. Kant, V. K. Gupta, G. B. Plata and J. M. Padrón, *New J. Chem.*, 2015, **39**, 2657–2668.
- 43 E. O. Terent'eva, A. S. Saidov, Z. S. Khashimova, N. E. Tseomashko, S. A. Sasmakov, D. M. Abdurakhmanov, V. I. Vinogradova and S. S. Azimova, *Chem. Nat. Compd.*, 2017, **53**, 328–332.
- 44 S. Murugesan, S. Ganguly and G. Maga, *J. Chem. Sci.*, 2010, **122**, 169–176.
- 45 J. J. Kennedy-Smith, N. Arora, J. R. Billedeau, J. Fretland, J. Q. Hang, G. M. Heilek, S. F. Harris, D. Hirschfeld, H. Javanbakht, Y. Li, W. Liang, R. Roetz, M. Smith, G. Su, J. M. Suh, A. G. Villaseñor, J. Wu, D. Yasuda, K. Klumpp and Z. K. Sweeney, *MedChemComm*, 2010, **1**, 79–83.
- 46 P. Zhan, W. Chen, Z. Li, X. Li, X. Chen, Y. Tian, C. Pannecouque, E. De Clercq and X. Liu, *Bioorg. Med. Chem.*, 2012, **20**, 6795–6802.
- 47 Schrödinger, *Schrödinger Release 2018-1*, 2018.
- 48 S. Chander, P. Ashok, A. Singh and S. Murugesan, *Chem. Cent. J.*, 2015, **9**, 1–13.
- 49 Y. Liao, Y. Ye, S. Li, Y. Zhuang, L. Chen, J. Chen, Z. Cui, L. Huo, S. Liu and G. Song, *Eur. J. Med. Chem.*, 2020, **189**, 112048.
- 50 W. A. Guiguemde, A. A. Shelat, D. Bouck, S. Duffy, G. J. Crowther, P. H. Davis, D. C. Smithson, M. Connelly, J. Clark, F. Zhu, M. B. Jiménez-Díaz, M. S. Martinez, E. B. Wilson, A. K. Tripathi, J. Gut, E. R. Sharlow, I. Bathurst, F. El Mazouni, J. W. Fowble, I. Forquer, P. L. McGinley, S. Castro, I. Angulo-Barturen, S. Ferrer, P. J. Rosenthal, J. L. Derisi, D. J. Sullivan, J. S. Lazo, D. S. Roos, M. K. Riscoe, M. A. Phillips, P. K. Rathod, W. C. Van Voorhis, V. M. Avery and R. K. Guy, *Nature*, 2010, **465**, 311–315.
- 51 D. M. Floyd, P. Stein, Z. Wang, J. Liu, S. Castro, J. A. Clark, M. Connelly, F. Zhu, G. Holbrook, A. Matheny, M. S. Sigal, J. Min, R. Dhinakaran, S. Krishnan, S. Bashyum, S. Knapp and R. K. Guy, *J. Med. Chem.*, 2016, **59**, 7950–7962.
- 52 M. B. Jiménez-Díaz, D. Ebert, Y. Salinas, A. Pradhan, A. M. Lehane, M. E. Myrand-Lapierre, K. G. O'Loughlin, D. M. Shackelford, M. J. De Almeida, A. K. Carrillo, J. A. Clark, A. S. M. Dennis, J. Diep, X. Deng, S. Duffy, A. N. Endsley, G. Fedewa, W. A. Guiguemde, M. G. Gómez, G. Holbrook, J. Horst, C. C. Kim, J. Liu, M. C. S. Lee, A. Matheny, M. S. Martínez, G. Miller, A. Rodríguez-Alejandre, L. Sanz, M. Sigal, N. J. Spillman, P. D. Stein, Z. Wang, F. Zhu, D. Waterson, S. Knapp, A. Shelat, V. M. Avery, D. A. Fidock, F. J. Gamo, S. A. Charman, J. C. Mirsalis, H. Ma, S. Ferrer, K. Kirk, I. Angulo-Barturen, D. E. Kyle, J. L. Derisi, D. M. Floyd and R. K. Guy, *Proc. Natl. Acad. Sci. U. S. A.*, 2014, **111**, E5455–E5462.
- 53 A. H. Gaur, J. S. McCarthy, J. C. Panetta, R. H. Dallas, J. Woodford, L. Tang, A. M. Smith, T. B. Stewart, K. C. Branum, B. B. Freeman, N. D. Patel, E. John, S. Chalon, S. Ost, R. N. Heine, J. L. Richardson, R. Christensen, P. M. Flynn, Y. Van Gessel, B. Mitasev, J. J. Möhrle, F. Gusovsky, L. Bebrevska and R. K. Guy, *Lancet Infect. Dis.*, 2020, **20**, 964–975.
- 54 J. N. Hanna, F. Ntie-Kang, M. Kaiser, R. Brun and S. M. N. Efang, *RSC Adv.*, 2014, **4**, 22856–22865.
- 55 H. M. Malebo, S. D'alessandro, Y. A. Ebstie, H. Sorè, A. R. T. Guedoung, S. J. Katani, S. Parapini, D. Taramelli and A. Habluetzel, *Drug Des., Dev. Ther.*, 2020, **14**, 1593–1607.
- 56 K. Chauhan, M. Sharma, R. Shivahare, U. Debnath, S. Gupta, Y. S. Prabhakar and P. M. S. Chauhan, *ACS Med. Chem. Lett.*, 2013, **4**, 1108–1113.
- 57 S. Chander, P. Ashok, R. M. Reguera, M. Y. Perez-Pertejo, R. Carbajo-Andres, R. Balana-Fouce, K. V. Gowri Chandra Sekhar and M. Sankaranarayanan, *Exp. Parasitol.*, 2018, **189**, 49–60.



- 58 D. R. Cullen, J. Pengon, R. Rattanajak, J. Chaplin, S. Kamchongwongpaisan and M. Mocerino, *ChemistrySelect*, 2016, **1**, 4533–4538.
- 59 P. S. Sadhu, S. N. Kumar, M. Chandrasekharam, L. Picamattocchia, D. Cioli and V. J. Rao, *Bioorg. Med. Chem. Lett.*, 2012, **22**, 1103–1106.
- 60 W. W. Duan, S. J. Qiu, Y. Zhao, H. Sun, C. Qiao and C. M. Xia, *Bioorg. Med. Chem. Lett.*, 2012, **22**, 1587–1590.
- 61 L. Dong, W. Duan, J. Chen, H. Sun, C. Qiao and C. M. Xia, *PLoS One*, 2014, **9**, e112163.
- 62 X. Wang, D. Yu, C. Li, T. Zhan, T. Zhang, H. Ma, J. Xu and C. Xia, *Parasites Vectors*, 2019, **12**, 1–13.
- 63 Z. X. Wang, J. L. Chen and C. Qiao, *Chem. Biol. Drug Des.*, 2013, **82**, 216–225.
- 64 W. L. Wang, L. J. Song, X. Chen, X. R. Yin, W. H. Fan, G. P. Wang, C. X. Yu and B. Feng, *Molecules*, 2013, **18**, 9163–9178.
- 65 S. Guglielmo, D. Cortese, F. Vottero, B. Rolando, V. P. Kommer, D. L. Williams, R. Fruttero and A. Gasco, *Eur. J. Med. Chem.*, 2014, **84**, 135–145.
- 66 G. Rai, C. J. Thomas, W. Leister and D. J. Maloney, *Tetrahedron Lett.*, 2009, **50**, 1710–1713.
- 67 H. M. Alger, A. A. Sayed, M. J. Stadecker and D. L. Williams, *Int. J. Parasitol.*, 2002, **32**, 1285–1292.
- 68 A. Gasco and K. Schoenafinger, in *Nitric Oxide Donors*, Wiley-VCH Verlag GmbH & Co. KGaA, Weinheim, FRG, 2005, pp. 131–175.
- 69 A. A. Sayed, A. Simeonov, C. J. Thomas, J. Inglese, C. P. Austin and D. L. Williams, *Nat. Med.*, 2008, **14**, 407–412.
- 70 A. Wąsik, E. Mozdzeń, I. Romańska, J. Michaluk and L. Antkiewicz-Michaluk, *Eur. J. Pharmacol.*, 2013, **700**, 110–117.
- 71 A. Patsenka and L. Antkiewicz-Michaluk, *Pol. J. Pharmacol.*, 2004, **56**, 727–734.
- 72 L. Antkiewicz-Michaluk, A. Wąsik and J. Michaluk, *Neurotoxic. Res.*, 2014, **25**, 1–12.
- 73 L. Antkiewicz-Michaluk, J. Michaluk, M. Mokrosz, I. Romanska, E. Lorenc-Koci, S. Ohta and J. Vetulani, *J. Neurochem.*, 2001, **78**, 100–108.
- 74 M. Maes, R. Yirmiyia, J. Noraberg, S. Brene, J. Hibbeln, G. Perini, M. Kubera, P. Bob, B. Lerer and M. Maj, *Metab. Brain Dis.*, 2009, **24**, 27–53.
- 75 L. Antkiewicz-Michaluk, J. W. Lazarewicz, A. Patsenka, M. Kajta, E. Ziemska, E. Salinska, A. Wasik, K. Golembiowska and J. Vetulani, *J. Neurochem.*, 2006, **97**, 846–856.
- 76 E. Mozdzeń, M. Papp, P. Gruca, A. Wąsik, I. Romańska, J. Michaluk and L. Antkiewicz-Michaluk, *Eur. J. Pharmacol.*, 2014, **729**, 107–115.
- 77 E. Mozdzeń, A. Wąsik, I. Romańska, J. Michaluk and L. Antkiewicz-Michaluk, *Pharmacol. Rep.*, 2017, **69**, 566–574.
- 78 A. Wąsik, E. Mozdzeń, J. Michaluk, I. Romańska and L. Antkiewicz-Michaluk, *Neurotoxic. Res.*, 2014, **25**, 323–334.
- 79 E. Mozdzeń, I. Babińska, J. Wójcikowski and L. Antkiewicz-Michaluk, *Pharmacol. Rep.*, 2019, **71**, 1140–1146.
- 80 B. Habibi, J. P. Cartron, M. Bretagne, P. Rouger and C. Salmon, *Vox Sang.*, 1981, **40**, 79–84.
- 81 J. H. Harrison and D. J. Jollow, *J. Pharmacol. Exp. Ther.*, 1986, **238**, 1045–1054.
- 82 J. Yu, D. G. Brown and D. Burdette, *Drug Metab. Dispos.*, 2010, **38**, 1767–1778.
- 83 A. D. Pechulis, J. P. Beck, M. A. Curry, M. A. Wolf, A. E. Harms, N. Xi, C. Opalka, M. P. Sweet, Z. Yang, A. S. Vellekoop, A. M. Klos, P. J. Crocker, C. Hassler, M. Laws, D. B. Kitchen, M. A. Smith, R. E. Olson, S. Liu and B. F. Molino, *Bioorg. Med. Chem. Lett.*, 2012, **22**, 7219–7222.
- 84 S. Liu, C. Zha, K. Nacro, M. Hu, W. Cui, Y. L. Yang, U. Bhatt, A. Sambandam, M. Isherwood, L. Yet, M. T. Herr, S. Ebeltoft, C. Hassler, L. Fleming, A. D. Pechulis, A. Payen-Fornicola, N. Holman, D. Milanowski, I. Cotterill, V. Mozhaev, Y. Khmel'nitsky, P. R. Guzzo, B. J. Sargent, B. F. Molino, R. Olson, D. King, S. Lelas, Y. W. Li, J. Kim, T. Molski, A. Orie, A. Ng, R. Haskell, W. Clarke, R. Bertekap, J. Oconnell, N. Lodge, M. Sinz, S. Adams, R. Zaczek and J. E. Macor, *ACS Med. Chem. Lett.*, 2014, **5**, 760–765.
- 85 D. K. Sukumarapillai, K. Kooi-Yeong, Y. Kia, V. Murugaiyah and S. K. Iyer, *Med. Chem. Res.*, 2016, **25**, 1705–1715.
- 86 N. Sudhapriya, A. Manikandan, M. R. Kumar and P. T. Perumal, *Bioorg. Med. Chem. Lett.*, 2019, **29**, 1308–1312.
- 87 N. Ghamari, O. Zarei, D. Reiner, S. Dastmalchi, H. Stark and M. Hamzeh-Mivehroud, *Chem. Biol. Drug Des.*, 2019, **93**, 832–843.
- 88 N. Ghamari, S. Dastmalchi, O. Zarei, J. A. Arias-Montañó, D. Reiner, F. Ustun-Alkan, H. Stark and M. Hamzeh-Mivehroud, *Chem. Biol. Drug Des.*, 2020, **95**, 279–290.
- 89 A. D. Medhurst, A. R. Atkins, I. J. Beresford, K. Brackenborough, M. A. Briggs, A. R. Calver, J. Cilia, J. E. Cluderay, B. Crook, J. B. Davis, R. K. Davis, R. P. Davis, L. A. Dawson, A. G. Foley, J. Gartlon, M. I. Gonzalez, T. Heslop, W. D. Hirst, C. Jennings, D. N. C. Jones, L. P. Lacroix, A. Martyn, S. Ociepka, A. Ray, C. M. Regan, J. C. Roberts, J. Schogger, E. Southam, T. O. Stean, B. K. Trail, N. Upton, G. Wadsworth, J. A. Wald, T. White, J. Witherington, M. L. Woolley, A. Worby and D. M. Wilson, *J. Pharmacol. Exp. Ther.*, 2007, **321**, 1032–1045.
- 90 D. Vohora and M. Bhowmik, *Front. Syst. Neurosci.*, 2012, 1–27.
- 91 Y. Chen, C. Su, L. Wang, J. Qin, S. Wei and H. Tang, *Mol. Diversity*, 2019, **23**, 709–722.
- 92 Y. Fang, H. Zhou, Q. Gu and J. Xu, *Eur. J. Med. Chem.*, 2019, **167**, 133–145.
- 93 Z. Pu, S. Ma, L. Wang, M. Li, L. Shang, Y. Luo and W. Chen, *Amyloid-beta Degradation and Neuroprotection of Dauricine Mediated by Unfolded Protein Response in a Caenorhabditis elegans Model of Alzheimer's disease*, 2018, vol. 392.
- 94 L. Wang, Z. Pu, M. Li, K. Wang, L. Deng and W. Chen, *Life Sci.*, 2020, **243**, 1–8.
- 95 P. Liu, X. Chen, H. Zhou, L. Wang, Z. Zhang, X. Ren, F. Zhu, Y. Guo, X. Huang, J. Liu, P. S. Spencer and X. Yang, *Oxid. Med. Cell. Longevity*, 2018, **2018**, 2025914.
- 96 L. Antkiewicz-Michaluk, J. Michaluk, M. Mokrosz, I. Romanska, E. Lorenc-Koci, S. Ohta and J. Vetulani, *J. Neurochem.*, 2001, **78**, 100–108.



## Review

- 97 A. Wąsik, I. Romańska and L. Antkiewicz-Michaluk, *Neurotoxic. Res.*, 2009, **15**, 15–23.
- 98 S. Shavali and M. Ebadi, *Neurotoxicology*, 2003, **24**, 417–424.
- 99 Y. Kotake, Y. Tasaki, Y. Makino, S. Ohta and M. Hirobe, *J. Neurochem.*, 1995, **65**, 2633–2638.
- 100 Y. Kotake, S. Ohta, I. Kanazawa and M. Sakurai, *Neuroscience*, 2003, **117**, 63–70.
- 101 R. Kohta, Y. Kotake, T. Hosoya, T. Hiramatsu, Y. Otsubo, H. Koyama, Y. Hirokane, Y. Yokoyama, H. Ikeshoji, K. Oofusa, M. Suzuki and S. Ohta, *J. Neurochem.*, 2010, **114**, 1291–1301.
- 102 A. Wąsik, I. Romańska, J. Michaluk, A. Zelek-Molik, I. Nalepa and L. Antkiewicz-Michaluk, *Neurotoxic. Res.*, 2016, **29**, 351–363.
- 103 A. Wąsik, I. Romańska and L. Antkiewicz-Michaluk, *Neurotoxic. Res.*, 2016, **30**, 648–657.
- 104 A. Wąsik, D. Polak, I. Romańska, J. Michaluk and L. Antkiewicz-Michaluk, *Pharmacol. Rep.*, 2016, **68**, 1205–1213.
- 105 A. Wąsik, I. Romańska, A. Zelek-Molik and L. Antkiewicz-Michaluk, *Neurotoxic. Res.*, 2018, **33**, 523–531.
- 106 N. Katagiri, S. Chida, K. Abe, H. Nojima, M. Kitabatake, K. Hoshi, Y. Horiguchi and K. Taguchi, *Brain Res.*, 2010, **1321**, 133–142.
- 107 K. Saitoh, K. Abe, T. Chiba, N. Katagiri, T. Saitoh, Y. Horiguchi, H. Nojima and K. Taguchi, *Pharmacol. Rep.*, 2013, **65**, 1204–1212.
- 108 H. J. Son, J. A. Lee, N. Shin, J. H. Choi, J. W. Seo, D. Y. Chi, C. S. Lee, E. M. Kim, H. Choe and O. Hwang, *Br. J. Pharmacol.*, 2012, **165**, 2213–2227.
- 109 H. J. Son, S. H. Han, J. A. Lee, C. S. Lee, J. W. Seo, D. Y. Chi and O. Hwang, *Eur. J. Pharmacol.*, 2016, **771**, 152–161.
- 110 H. Sun, X. He, C. Liu, L. Li, R. Zhou, T. Jin, S. Yue, D. Feng, J. Gong, J. Sun, J. Ji and L. Xiang, *ACS Chem. Neurosci.*, 2017, **8**, 155–164.

